frontiers | Frontiers in Earth Science

TYPE Original Research
PUBLISHED 01 May 2024
DOI 10.3389/feart.2024.1396061

OPEN ACCESS

EDITED BY
Shuai Yin,
Xi'an Shiyou University, China

REVIEWED BY
Junjie Lu,
Jilin University, China
Tianjia Liu,
SINOPEC Petroleum Exploration and Production Research Institute, China

*CORRESPONDENCE
Dandan Hu,
hdd_0619@163.com

RECEIVED 05 March 2024
ACCEPTED 09 April 2024
PUBLISHED 01 May 2024

CITATION
Li W, Hu D, Gong C, Fan T, Chen Y, Li Y, Shi Q and Leng Q (2024), Controlling factors of high-quality reservoirs in low permeability sandstone: a case study of the upper member of the lower Ganchaigou formation, Qaidam basin.
Front. Earth Sci. 12:1396061.
doi: 10.3389/feart.2024.1396061

Controlling factors of high-quality reservoirs in low permeability sandstone: a case study of the upper member of the lower Ganchaigou formation, Qaidam basin

Wenhuan Li[1], Dandan Hu[1]*, Changli Gong[2], Tailiang Fan[3], Yihang Chen[1], Ya'nan Li[4], Qi Shi[4] and Qifeng Leng[1]

[1]Research Institute of Petroleum Exploration and Development, PetroChina, Beijing, China, [2]China National Oil and Gas Exploration and Development Company Ltd., Beijing, China, [3]China University of Geosciences, Beijing, China, [4]Research Institute of Exploration and Development of Qinghai Oilfield Company, PetroChina, Dunhuang, China

The upper member of the Lower Ganchaigou Formation (UMoLGF) is a high-potential hydrocarbon exploration area in the North margin of the Qaidam Basin (NMoQB). It represents a typical low-permeability sandstone reservoir. The current understanding of reservoir characteristics of the UMoLGF is poor, and the main controlling factors of high-quality reservoir development remaining unclear. This study, for the first time, integrated various factors to investigate the formation mechanism of high-quality reservoirs in the UMoLGF's low-permeability sandstone reservoirs. Results show three provenance systems developed in the study area: northwest, northeast, and east. The northwestern and northeastern areas share similar reservoir characteristics. The rock type is predominantly feldspar, with relatively poor particle sorting and rounding. Pore types are dominated by secondary dissolution pores. However, the northwestern area has more developed fractures and poorer pore structures than the northeastern. Meanwhile, in the eastern area, the rock fragment content was high, the rock type was mainly litharentie and lithic arkose, particles were well-sorted and well-rounded. Residual intergranular pores, with good structures, dominated the pore type. The UMoLGF has entered the eo-diagenesis B stage with minor progression into the meso-diagenesis A stage. Based on quantitive calculations, this study established porosity evolution models for the different study areas. The initial porosities in the northwestern, northeastern, and eastern areas were 30.8%, 30.4%, and 34.8%, respectively. Compaction and cementation are the major factors contributing to porosity reduction in the three areas, with the most significant impact in the northwestern area. Dissolution significantly improved the reservoir properties in the northwestern area, with little effect on the northeastern and eastern areas. The formation of high-quality reservoir in the UMoLGF was affected by provenance, diagenesis, and fractures, with the primary controlling factors varying by area. In the northwestern area, the formation of high-quality reservoirs benefited from strong dissolution and well-developed fractures. In the northeastern area, the high-quality reservoir was relied upon favorable provenance and dissolution. In the eastern area, provenance provided an

excellent material basis for developing high-quality reservoirs, with dissolution and chlorite cementation further improving reservoir properties. This study provides a theoretical foundation for further exploration and development of UMoLGF and offers insights for exploring and developing similar low-permeability sandstone reservoirs.

KEYWORDS

formation mechanism, high-quality reservoir, low-permeability sandstone reservoir, upper member of the lower Ganchaigou formation, Qaidam basin

1 Introduction

With the increasing global energy demand, low-permeability reservoirs have received considerable attention in recent years owing to their large oil and gas resource potential (Hu, 2009; Liu et al., 2016; Hu et al., 2018; Wang et al., 2018; Li H. et al., 2019). Approximately 38% of the world's hydrocarbon resources originates from low-permeability reservoirs (Hu et al., 2018; Xie et al., 2022); accordingly, the low-permeability oil and gas fields are becoming increasingly important for global hydrocarbon development (Cao et al., 2018; Hu et al., 2018; Xie et al., 2023). However, owing to varying policies, resources, and technological levels among countries, a uniform definition for low-permeability reservoirs has not been established (Chen et al., 2019). In China, sandstone reservoirs with a permeability of ≤50 mD are defined as low-permeability sandstone reservoirs (Yang et al., 2007; Hu, 2009; Cao et al., 2018). These reservoirs are mainly distributed in the Songliao, Ordos, Qaidam, Junggar, Sichuan, Tarim and other basins (Hu, 2009; Zou et al., 2015; Hu et al., 2018; Wang, et al., 2018). Among these basins, the low-permeability reserves in Songliao, Ordos, Qaidam, and Junggar basins account for ≥85% of the total reserves (Hu et al., 2018).

Low-permeability sandstone reservoirs are characterized by strong heterogeneity, complex pore structures, small pore throats, poor connectivity, and complex seepage mechanisms (Zou et al., 2015; Cao et al., 2018; Wang, et al., 2018; Xie et al., 2023). Reservoir quality varies significantly in horizontal and vertical dimensions. Low permeability is the bottleneck restricting the effective development of low-permeability sandstone reservoirs. Hence, identifying high-quality reservoirs against a background of low permeability remains a significant challenge warranting urgent attention. High-quality low-permeability sandstone reservoirs refer to those with relatively good porosity and permeability (Wang et al., 2003; Zou et al., 2009). Low-permeability sandstone reservoirs typically develop high-quality reservoirs, making them ideal for exploration and development (Zou et al., 2013; Gao et al., 2018; Wu et al., 2019). However, in-depth analyses are needed to clarify the characteristics and the formation mechanisms of low-permeability and high-quality reservoirs, and to predict the distribution of high-quality reservoirs (Zou et al., 2013; Liu et al., 2016; Cao et al., 2018; Chen et al., 2019).

Previous studies have identified key factors regulating the development of high-quality reservoirs in low-permeability sandstone reservoirs, including the sedimentary environment, tectonic movement, diagenesis, and hydrocarbon filling (Wang et al., 2003; Zou et al., 2009; Yang et al., 2014; Liu et al., 2016; Zhou et al., 2017; Cui et al., 2019; Bai et al., 2021; Xie et al., 2023). Regarding the sedimentary environment, sand bodies formed in high-energy sedimentary environments tend to possess significant sedimentary thickness, low matrix content, high compositional maturity, coarse grain size, good sorting, high structural maturity, and high initial porosity (Zheng et al., 2007; Bjørlykke, 2014; Zhou et al., 2017). These sand bodies exhibit an anti-compaction capacity and can maintain well-connected primary pores before undergoing dissolution transformation. The dominant sedimentary environment is often a favorable zone for developing high-quality reservoirs (Zhou et al., 2017; Cao et al., 2018; Li S. S. et al., 2019). Meanwhile, dissolution is the primary diagenetic process that contributes to high-quality reservoirs. Based on different dissolution mechanisms, such as thermal evolution of organic matter, carbonate-clay reaction, atmospheric freshwater leaching, and clay mineral transformation (Bjørlykke, 1993; Huang et al., 2003; Guo et al., 2009; Taylor et al., 2010; Zhao et al., 2015). For low-permeability sandstone reservoirs, the secondary pores formed by dissolution are essential controlling factors for developing high-quality reservoirs. Tectonic movements can create fractures, serving as channels for fluid flow and reservoir space for oil and gas. Faults and unconformities caused by these movements can also act as channels for organic acids, atmospheric fresh water, and deep hydrothermal fluids (Shi et al., 2003; Jiang et al., 2015; Zhu et al., 2018). These channels aid the dissolution of nearby sandstone and the formation of secondary pores. Hydrocarbon filling can alter the pore fluid composition, inhibiting diagenesis to varying degrees (Masst et al., 2011; Ji et al., 2015). Early hydrocarbon filling can effectively slow the reduction of porosity caused by compaction and cementation, which is conducive to forming high-quality reservoirs (Bjørkum et al., 1993; Worden et al., 2018).

The upper member of the Lower Ganchaigou Formation (UMoLGF) is the key oil and gas exploration strata in the northern margin of the Qaidam Basin (NMoQB). It is characterized by various sedimentary facies, multi-provenance systems, complex diagenesis, and frequent tectonic movement. Although the UMoLGF represents a typical low-permeability sandstone reservoir, some areas have developed high-quality reservoirs with excellent porosity and permeability. Predecessors have conducted a lot of research on the factors affecting the development of the high-quality reservoirs in the UMoLGF. For example, Li et al. (2009) posited that rock composition and diagenesis significantly affect reservoir quality in the NMoQB. Sun et al. (2012) reported that diagenesis is the primary factor impacting the reservoir quality. In contrast, Chen et al. (2013) and Jia et al. (2014) proposed that sedimentary facies determine the reservoir quality in the NMoQB. However, these studies typically focused on single factors, resulting in one-sided conclusions. Overall, the current understanding of the reservoir characteristics of

the UMoLGF remains relatively inadequate, and the primary factors impacting high-quality reservoir development in different areas are unclear. Thus, hydrocarbon exploration of the low-permeability sandstone reservoirs in this area is hindered.

Based on various analytical test data, this study is the first to integrated multiple factors (such as deposition, diagenesis, and tectonic processes) to explore the main controlling factors of high-quality reservoir development of low-permeability sandstone reservoirs within the UMoLGF. As such, the primary objectives of this study are to (a) analyze the provenance systems of the UMoLGF within the study area; (b) compare the reservoir characteristics in different areas; (c) clarify the diagenetic characteristics and establish porosity evolution models for the different areas of the UMoLGF; and (d) clarify the primary factors impacting the high-quality reservoir formation in different areas of the UMoLGF.

Collectively, this study advances the current understanding regarding the formation mechanism of the high-quality reservoirs in the UMoLGF's low-permeability sandstone reservoirs and provides a theoretical foundation for further exploration and development within the area. Moreover, these insights can be applied to the exploration and development of similar low-permeability sandstone reservoirs.

2 Geological setting

Located in northwestern China, the Qaidam Basin is a large petroliferous basin that developed after the Indosinian movement (Sun et al., 2010; Pang et al., 2022). The basin's internal structure and sedimentary evolution were shaped by various tectonic movements, including the strike-slip movement of the Altyn Tagh Fault's, northward subduction of the Indian Plate, and the uplift of the Qinghai–Tibet Plateau. The basin is irregularly diamond-shaped, featuring a high elevation in the northwest and a low elevation in the southeast (Figure 1) (Li et al., 2022; Wang et al., 2023).

The Qaidam Basin has undergone various tectonic movements over time, including those of Caledonian, Hercynian, Indosinian, Yanshan, and Himalayan orogenies (Feng et al., 2022). The basin consists of three structural units (Figure 1) (Chen et al., 2008; Fu, 2014). The NMoQB is an essential area for hydrocarbon exploration with well-structured oil storage and a widely and continuously distributed caprock. In the 1950s, the Lenghu Oilfield was discovered in the NMoQB. More, recently, oil and gas fields have been discovered in succession, including Mabei, Nanbaxian, Niudong, and Pingtai, indicating that the NMoQB has a high exploration potential (Fu, 2014; Tian et al., 2020; Li et al., 2023). However, the overall exploration rate in this area is relatively low.

The Qaidam Basin has experienced substantial changes in its provenance, sedimentary center, and accumulation rate during the Cenozoic (Wang et al., 2023). Compared with other regions, the tectonic movements of the NMoQB in the Cenozoic was particularly complex and changeable. From the Paleogene to the early Pliocene, the NMoQB remained stable and located on the edge of the Qaidam Basin for a long time. During the middle to late Pliocene-Quaternary, the NMoQB underwent significant tectonic deformation due to the strengthening of the tectonic movement in the late Himalayan period. This deformation included intra-basin strike-slip, basin margin thrust, and old mountain uplift, eventually forming the current structural features of the NMoQB (Feng et al., 2022). Because of these complex tectonic movements, the NMoQB featured multi-provenance systems, substantial changes in the sedimentary environment, and complex factors controlling reservoir quality in the Cenozoic era (Ma et al., 2016; Sun et al., 2019).

Based on outcrop, stratigraphic correlation, fossil, drilling, and logging analyse, the Cenozoic formations in the Qaidam Basin have been classified into seven formations. From old to new are as follows: the Lulehe Formation (E_{1+2}), the Ganchaigou Formation including the Lower Member of Lower Ganchaigou Formation (E_3^1) and the UMoLGF (E_3^2), the Upper Ganchaigou Formation (N_1), the Youshashan Formation including the Lower Youshashan Formation (N_2^1) and the Upper Youshashan Formation (N_2^2), the Shizigou Formation (N_2^3), the Qigequan Formation (Q_{1+2}), and the Dabuxunyanqiao Formation (Q_{3+4}) (Figure 2) (Guan and Jian, 2013; Jian et al., 2018; Jian et al., 2024).

The study area within the NMoQB, with the Altun Mountains to the west and the Saishiteng, Xiaosaishiteng, and western Qilian Mountains to the north. It includes Niudong, Lenghu, Pingtai, Mabei, and Nanbaxian (Figure 1). The target layer located in the UMoLGF (Figure 2). The lower part of UMoLGF is mainly gray, yellow, and gray sandstone, with sandy mudstone and a small amount of argillaceous sandstone and siltstone. The upper part of UMoLGF is mainly gray, gray-green, brown, and gray sandstone, along with silt sandstone and sandy mudstone. As for the sedimentary environment, the Niudong, Lenghu, and platform areas developed fan delta–lacustrine systems, while the Mabei and Nanbaxian areas developed braided river delta–lacustrine systems.

3 Samples and methods

3.1 Materials

Samples from 25 wells were obtained from the UMoLGF. Heavy mineral, grain size, cast thin section (CTS), scanning electron microscopy (SEM), X-ray diffraction (XRD), high-pressure mercury injection, and physical analyses were conducted.

The Qinghai Oilfield Exploration and Development Research Institute shared data pertaining to the grain size for141 samples from 16 wells, the high-pressure mercury injection results for 69 samples from 15 wells, and the vitrinite reflectance (R_0) results for 15 samples from 5 wells.

3.2 Methods

3.2.1 XRD

To quantitatively analyze the clay mineral components and whole rock minerals of sandstones, 123 samples from 10 wells were selected for X-ray diffraction analysis (model: Empyrean Sharp Shadow). First, these samples were powdered using an agate mortar and a grinder, and then the clay fraction (<2 μm) was separated from the water based on the suspension method. The

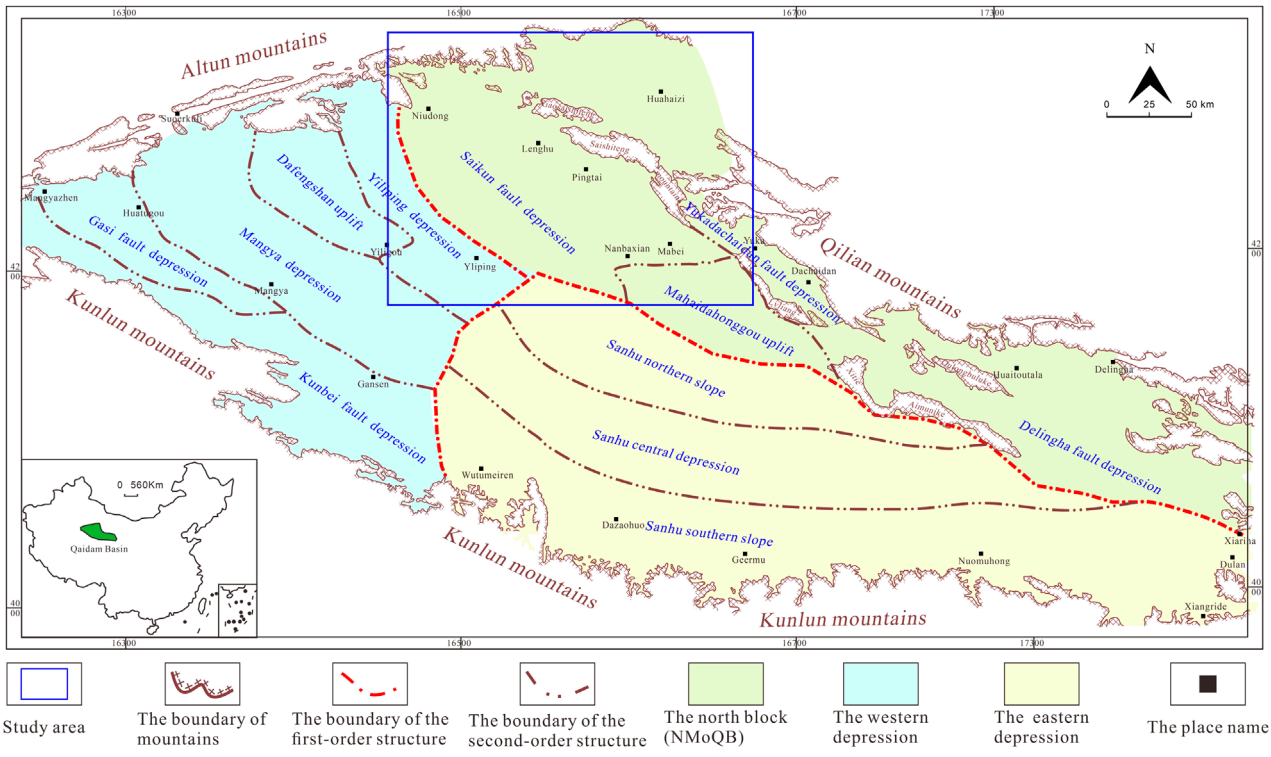

FIGURE 1
Map describing the structural units of the Qaidam Basin and marking location of the study area.

minerals composition can be deduced according to 550 °C heated and ethylene-glycol saturation diffractograms.

3.2.2 Heavy minerals

In total, 196 samples drilled from 25 wells were prepared for heavy mineral analysis. The samples were broken and fully dissolved with acid, followed by grinding and filtration. The sediment obtained after filtration was dried at 40 °C in an oven, then the fine sand composition was collected using a wet sieve. Subsequently, the dried samples were divided into heavy and light components with bromoform (2.89 g/cm^3). Various microscopes were used to identify light and heavy minerals, including binocular stereoscopes, polarizing microscopes, and microscopic analysis. This study utilized the strip number particle method to determine the percentage of light and heavy minerals present in each sample. The number of particles identified in each sample exceeded 300.

3.2.3 CTS

In total, 183 samples were collected from 15 wells and prepared for CTS observation. Blue-dyed epoxy resin was vacuum-impregnated into all the samples to visualize the pores. Alizarin red was used to stain the samples to identify carbonate minerals (red: calcite, purple: iron calcite, colorless: dolomite, and blue: iron dolomite). A polarizing microscope (Model: ZEISS imager. A2) was used to observe the thin sections. Point counting was used to determine debris composition, porosity, pore type, and structural characteristics, with 350 points per thin section.

3.2.4 Reservoir property

In total, 698 samples were collected from 15 wells to analyze the reservoir properties. They samples were made into cylinders with a 2.5 cm diameter. A porosity tester (Model: Ultra Pore-400) and a permeability tester (Model: DX-07G) were used to measure porosity and permeability, respectively.

3.2.5 SEM

SEM was utilized to identify the authigenic clay minerals and observe their pore structure and morphology. Gold-plated slices were prepared from 11 samples from five Wells and evaluated under an electron microscope (model: ZEISS EVO-18–18). Observed under high magnification, kaolinite, chlorite, and illite have distinct morphologies. Kaolinite typically presents a pseudo-hexahedron single mineral, and its aggregate is book-like or worm-like. Chlorite is needle-like or rose-like, and Illite is filamentous and flake. The illite-montmorillonite mixed layer is mainly in the forms of honeycomb and flake.

3.3 Quantitative analysis of porosity

Previous studies on pore evolution have mostly been qualitative analyses of diagenesis on reservoir control of the UMoLGF,

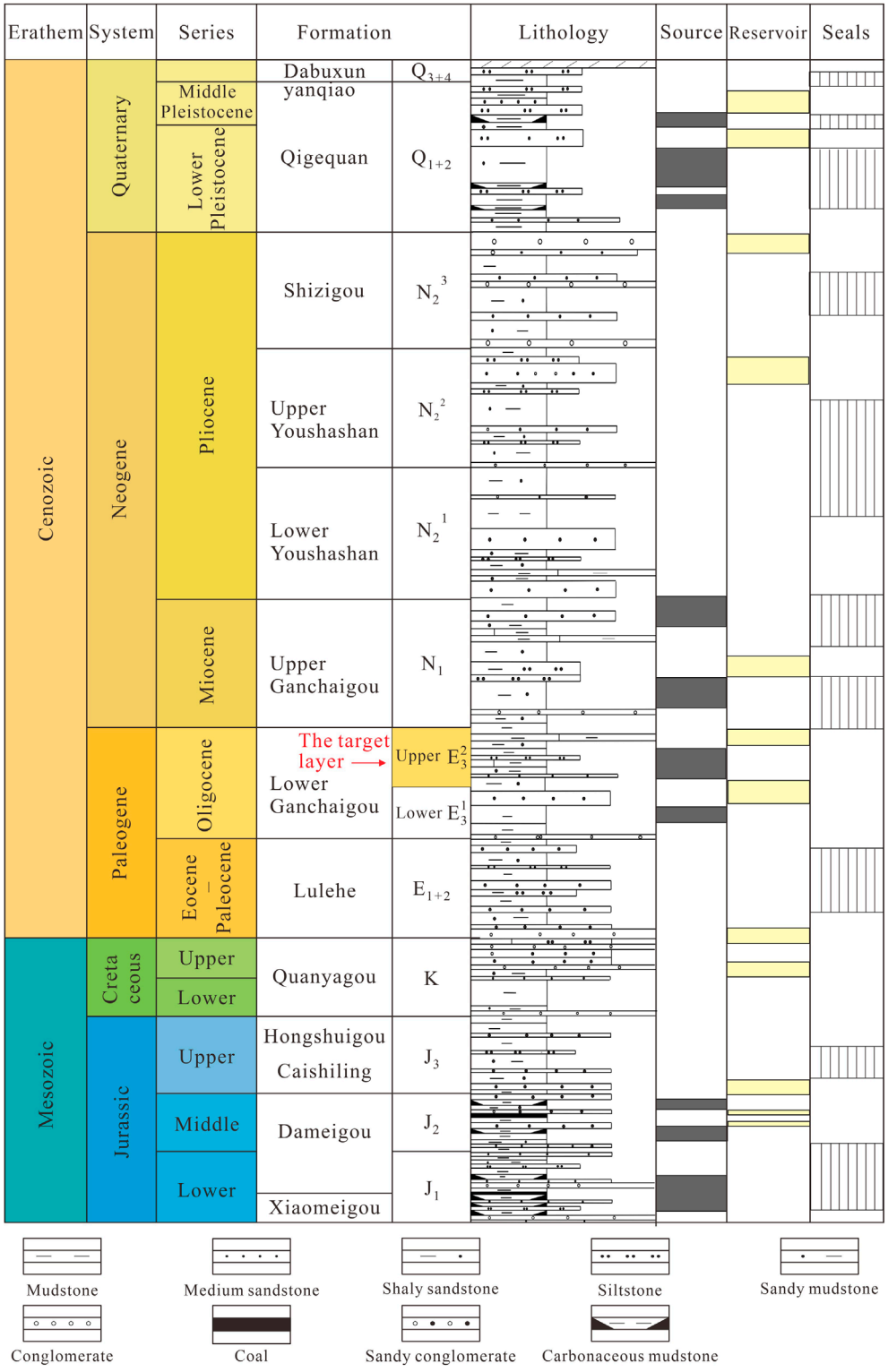

FIGURE 2
Mesozoic-Cenozoic stratigraphic column in the Qaidam Basin.

lacking quantitative analysis. Based on CTS observation and reservoir properties analysis, this study quantitatively characterized the effect of different diagenesis on reservoir quality. The equations for quantitative calculation for porosity evolution are presented in Table 1 (Beard and Weyl, 1973; Wang et al., 2017).

TABLE 1 Equations for quantitative calculation of porosity evolution.

Equations	Symbols in the equations
$\Phi_0 = 20.91 + \frac{22.90}{S_0}$	Φ_0: Initial porosity, %
$S_0 = \left[\frac{G_{25}}{G_{75}}\right]^{\frac{1}{2}}$	Φ_{com}:*Residual porosity after compaction*, %;
$\Phi_{com} = C + \frac{P_r}{P_t} \times P_{cor}$	Φ_{cem}:*Porosity after cementation*, %;
$R_{com} = \frac{(\Phi_0 - \Phi_{com})}{\Phi_0} \times 100\%$	Φ_{dis}:Porosity after dissolution, %
$\Phi_{cem} = \frac{P_r}{P_t} \times P_{cor}$	S_0: Sorting coefficient, f
$R_{cem} = \frac{(\Phi_{com} - \Phi_{cem})}{\Phi_0} \times 100\%$	C: Percentage of cements, %
$\Phi_{dis} = \frac{P_d}{P_t} \times P_{cor}$	G_{25}: Particle diameters at 25% of the cumulative size curve
$R_{dis} = \frac{(\Phi_{cem} - \Phi_{dis})}{\Phi_0} \times 100\%$	G_{75}: Particle diameters at 75% of the cumulative size curve
	P_{cor}: Core porosity, %
	P_r: Residual intergranular pores in the thin section, %
	P_d: Dissolution pores in the thin section, %
	P_t: Thin section porosity, %

4 Results

4.1 Provenance

The source rock type and transport distance of the provenance area directly determine the sediment composition. Heavy minerals are essential to sandstone debris, characterized by strong weathering resistance, wide distribution, and strong chemical stability (Weltje and Von Eynatten, 2004; Xu et al., 2021). They can retain the parent rock's characteristics more thoroughly when transporting and depositing with other sediments. Therefore, heavy minerals are an effective indicator of sediment provenance (Weltje and Von Eynatten, 2004; Xu et al., 2021; Yi et al., 2023). Fourteen heavy mineral types were detected in the UMoLGF, among which magnetite predominated. Thus, magnetite was excluded from the analysis to avoid errors, and other minerals were quantified according to their relative percentages.

In the Niudong area, the heavy minerals included zircon (31.6%), tourmaline (31.5%), and epidote (12.5%). In the Lenghu and Pingtai areas, the heavy minerals included garnet (33.1%), zircon (24.0%), epidote (13.8%), and white titanium (15.3%). In the Mabei and Nanbaxian areas, the heavy minerals primarily included garnet (42.5%), white titanium (30.0%), and zircon (18.2%). Based on the heavy mineral analysis, three provenances of the UMoLGF were identified: northwest, northeast, and east (Figure 3). The ultra-stable heavy mineral contents, such as zircon gradually decreased from west to east. Meanwhile, the contents of stable and moderately stable heavy minerals, such as garnet and epidote, gradually increased. Hence, the northwestern area wasFigure 3 the closest to the provenance, followed by the northeastern area. The eastern area is the farthest from the provenance.

4.2 Petrological characteristics

The sandstone components in the three areas exhibited slight differences. In the northwestern area, the feldspar (avg. 37.02%) and rock fragment (avg. 37.98%) contents were relatively high, and the quartz content is lower (avg. 25.00%). In the northeastern area, the contents of feldspar (avg. 38.82%) and quartz (avg. 32.23%) were similar, whereas the rock fragment content was relatively low (avg. 28.95%). In the eastern area, the quartz content was relatively high (avg. 41.49%), and the feldspar (28.84%) and debris (29.67%) contents were low. The northwestern and northeastern areas share similar petrological characteristics - mainly arkose, lithic arkose, and feldspathic litharenite, with high feldspar content. In the eastern area, the rock types are primarily feldspathic litharenite and lithc arkose, with a relatively high rock fragment content (Figure 4).

The particles in the northwestern and northeastern areas were mainly sub-angular. In contrast, the sandstone in the eastern area had a high level roundness, with sub-edges and sub-round shapes. Sorting in the northwest, northeast, and east was poor, medium–poor, and medium, respectively. The cementation throughout the study area was weak. The northwestern and northeastern areas were dominated by pore cementation, whereas the eastern area was dominated by pore and contact cementation.

4.3 Reservoir space

Reservoir space of the UMoLGF primarily included residual intergranular pores (RIPs), secondary dissolution pores, and fractures, with significant variation across the different areas (Table 2; Figure 5).

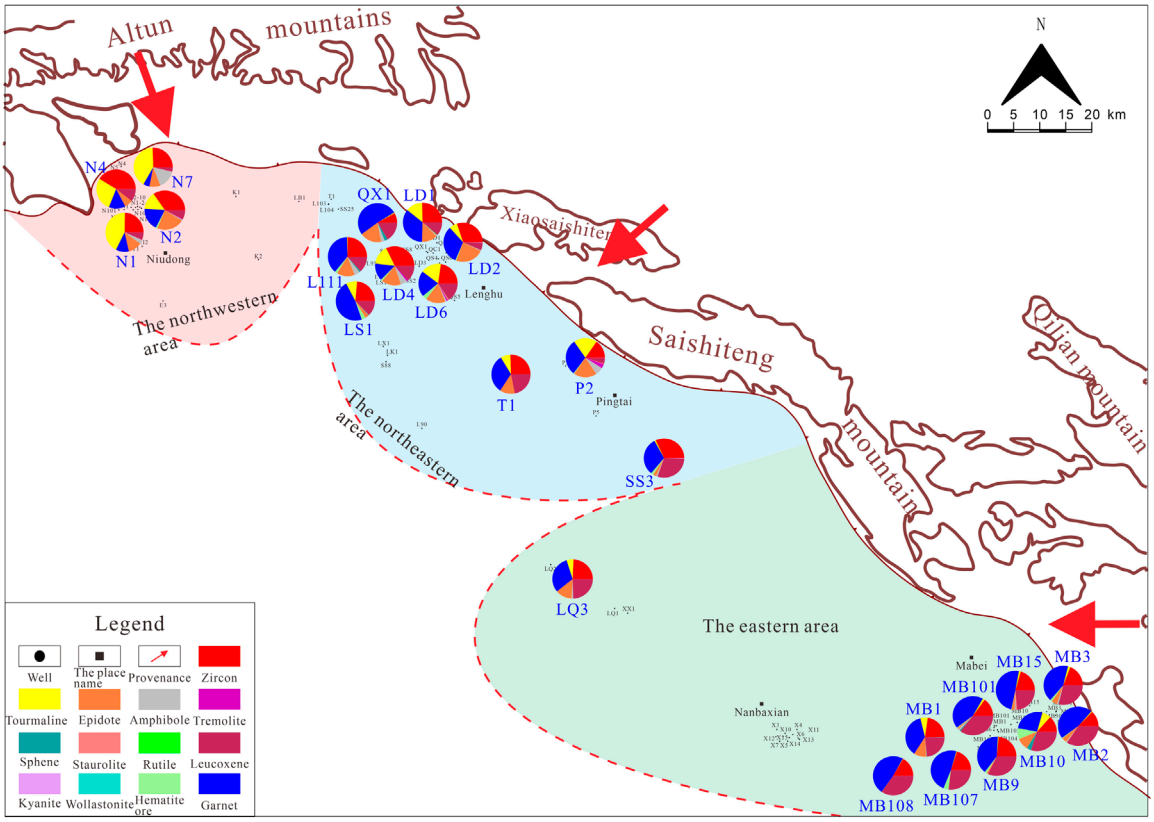

FIGURE 3
Heavy mineral distribution of the UMoLGF in the NmoQB.

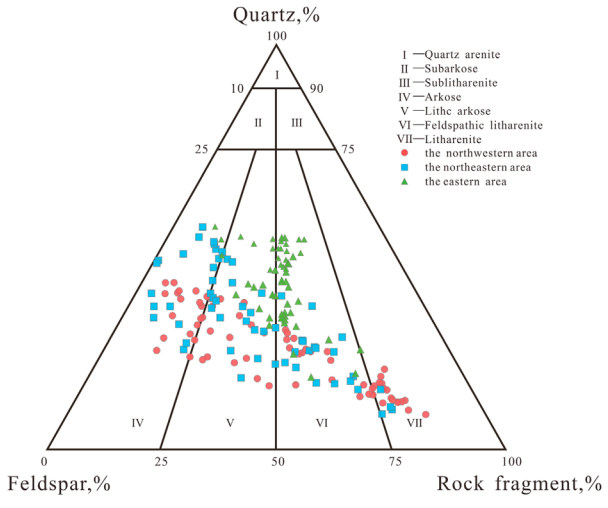

FIGURE 4
The ternary diagram of the UMoLGF in different areas.

4.3.1 RIPs

RIPs were widely distributed throughout the three areas; however, they were more developed within the eastern area, accounting for 91.4% of the thin section porosity. The RIPs in the eastern area were diverse in shape, with triangles, polygons, and irregular shapes. The pores were large and well connected with flat edges (Figures 5E, F). The RIP contents in the northwestern and northeastern were lower, accounting for 16.12% and 39% of the thin section porosity, respectively (Table 2), with fewer RIPs and with poor connectivity compared with those in the eastern area (Table 2; Figures 5D–F).

4.3.2 Secondary dissolution pores

This type of pore was critical in the UMoLGF and can be divided into intergranular and intragranular dissolution pores.

4.3.3 Intergranular dissolution pores

The intergranular dissolution pores were more developed in the northwestern and northeastern areas than in the eastern area (Table 2; Figure 5). CTS observations showed that the intergranular dissolution pores have an uneven distribution and high level of connectivity. The edges of the dissolved particles were typically irregular, jagged, or uneven.

4.3.4 Intragranular dissolution pores

The development of intragranular dissolution pores varied among the different areas, with the highest level in the northwest, followed by the northeastern and the eastern areas (Table 2). The CTS observations showed that these pores were mostly found in soluble particles, in the form of spots and honeycombs (Figure 5).

TABLE 2 The reservoir space types in different areas of the UMoLGF.

Area	Sample number	Pore types			Thin section porosity (%)	Frequency		
		Residual intergranular pores (%)	Secondary dissolution pores (%)	Fractures (%)		Residual intergranular pores (%)	Secondary dissolution pores (%)	Fractures (%)
The northwestern area	65	0.83	3.69	0.63	5.15	16.12	71.65	12.23
The northeastern area	53	2.17	3.29	0.02	5.48	39.60	60.04	0.36
The eastern area	58	11.63	1.09	1.09	12.72	91.43	8.57	0.00

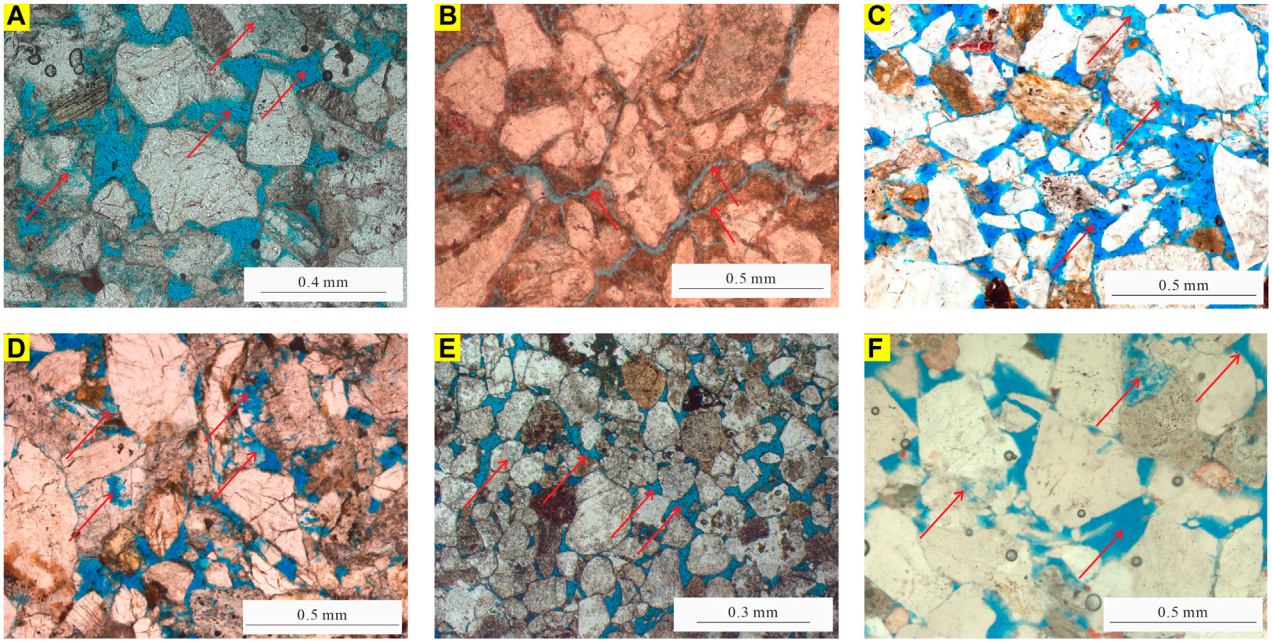

FIGURE 5
Reservoir space of the UMoLGF: **(A)** N3, 912.6 m, intergranular and intragranular dissolution pores; **(B)** N5, 789.24 m, intragranular dissolution pores, fractures; **(C)** L95, 1106.74 m, intergranular and intragranular dissolution pores; **(D)** Y2, 1414.6 m, RIP, intergranular and intragranular dissolution pores; **(E)** MB15, 1356.78 m, RIP, intragranular pores; **(F)** XX1, 4210.23 m, RIP, intergranular and intragranular dissolution pores. RIP = residual intergranular pore.

Carbonate cements, such as calcite cements, can be dissolved, forming some intragranular dissolution pores.

4.3.5 Fractures

Fractures occurred primarily in the northwestern area, characterized by a piedmont nose-like uplift. Multiple sets of fault systems developed under tectonic stress, resulting in the development of relatively well-developed structural fractures (Figure 5B). Fractures can serve as effective reservoir spaces and improve reservoir connectivity (Figure 5B). The fractures occasionally developed in the northeastern area but not the east.

Thin section porosities in the northwestern (5.15%) and northeastern (5.48%) areas were relatively similar (Table 2). The secondary dissolution pores dominated the reservoir space in these two areas, with thin section porosity of 3.69% and 3.29%, respectively (Table 2). However, fractures were more developed in the northwestern area, accounting for 12.23% of the thin section porosity (Table 2).

The thin section porosity of the eastern area reached12.72%, with the pore types in dominated by RIPs (91.43%) (Table 2), followed by secondary pores, (8.57%). Fractures were not developed (Table 2).

10.3389/feart.2024.1396061

TABLE 3 The Pore structure characteristics of UMoLGF in different areas.

Area	Sample number	Type	Frequency (%)	Porosity (%)	Permeability (mD)	Displacement pressure (Mpa)	Maximum pore throat radius (μm)	Maximum mercury saturation (%)	Saturation median pressure (Mpa)	Saturation median radius (μm)	Mercury withdrawal efficiency (%)
The northwestern area	31	I2	3.2	18.31	27.48	0.06	11.86	60.49	71.20	0.01	23.45
		II1	19.4	14.99	4.60	0.30	2.78	79.76	17.18	0.11	23.59
		II2	48.4	12.35	0.46	0.95	0.88	85.21	22.61	0.06	27.65
		III1	16.1	11.16	0.14	2.52	0.30	70.94	51.68	0.02	35.03
		III3	12.9	10.37	0.17	8.41	0.10	78.47	56.09	0.02	37.44
The northeastern area	16	I2	18.8	21.30	51.37	0.08	9.60	72.43	2.48	0.36	3.2915.06
		II1	37.5	20.25	15.17	0.29	6.23	74.52	7.28	0.13	21.47
		II2	31.3	14.84	0.54	0.97	0.81	73.02	22.49	0.04	28.84
		III1	12.5	11.65	0.19	2.90	0.26	73.07	20.87	0.04	26.86
The eastern area	22	I1	31.8	27.26	1390.99	0.03	29.35	83.69	0.07	11.86	4.13
		II1	40.9	8.59	1.00	0.29	3.23	85.90	1.90	0.47	20.01
		II2	27.3	6.99	0.20	1.22	0.64	78.49	12.12	0.16	22.58

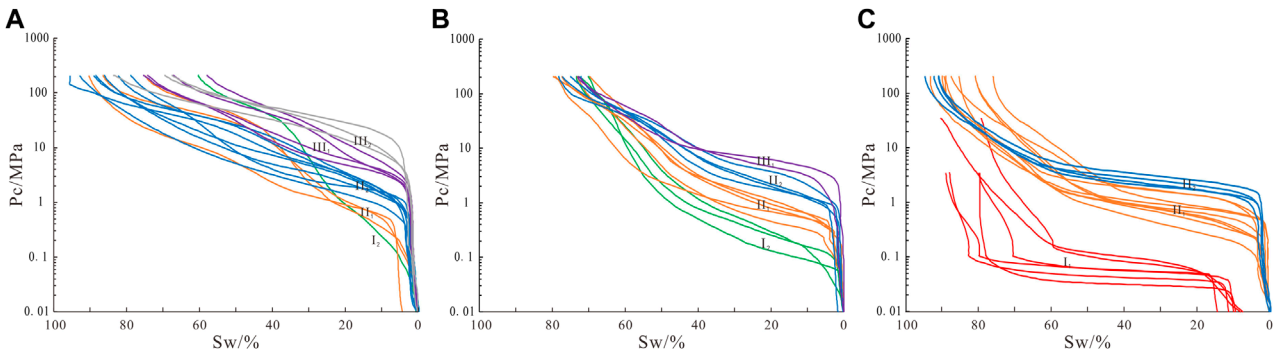

FIGURE 6
The capillary pressure curves in the **(A)** northwestern, **(B)** northeastern, and **(C)** eastern areas.

4.4 Pore structure characteristics

High-pressure mercury injection is effective for studying pore-throat structures (Zhang et al., 2017; Zhang et al., 2021). Based on reservoir classification standard of China (SY/T 6285–2011), the pore-throat structural of the UMoLGF was analyzed using displacement pressure (Pd) and the median pore throat radius (R_{50}) as the primary classification principle and combining the characteristics of the capillary pressure curve (CPC). The pore structure of the UMoLGF was classified into three types and six subtypes (Table 3; Figure 6).

Type I1 is characterized by ultra-low displacement pressure (Pd < 0.05) and ultra-fine throat (R50 ≥ 25.0). The CPC was central and exhibited a coarse distortion. The reservoir corresponding to type I1 was the best of the UMoLGF. The pore types were dominated by RIPs, followed by secondary dissolution pores. The pores were well-developed with good connectivity.

Type I2 has ultra-low displacement pressure (0.05 ≤ Pd < 0.1) and an ultra-fine throat (15.0 ≤ R50 < 25.0). The CPC had a slight inclination toward the lower left with a rough skewness. The corresponding reservoir space primarily consisted of RIPs and intergranular dissolution pores with well-developed pores and pore connectivity.

Type II1 was featured with a low displacement pressure (0.1 ≤ Pd < 0.5) and an ultra-fine throat (5.0 ≤ R50 < 15.0) (Table 3). The CPC exhibited a minor leftward and slightly rough skewness. The corresponding reservoir space primarily consisted of RIPs and intergranular dissolution pores with moderate pore structures.

Type II2 had the characteristics of medium displacement pressure (0.5 ≤ Pd < 2) and an ultra-fine throat (3.0 ≤ R50 < 5.0) (Table 3). The CPC was central and slightly skewed. The corresponding reservoir space was mainly secondary dissolution pores with poor pore connectivity.

Type III1 was characterized by high displacement pressure (2.0 ≤ Pd < 5.0) and an ultra-fine throat (R50 < 3) (Table 3). The CPC was slightly inclined toward the upper right with slight skewness. The corresponding reservoir developed a few RIPs with poor pore connectivity.

Type III2 was characterized by ultra-high displacement pressure (Pd ≥ 5) with no observable (Table 3). The CPC was generally finely skewed to the upper right.

The mercury injection results revealed significant differences in pore structure among the three areas.

The northwestern area: Five types of pore-throat structures have developed. Type II2 was the most developed (48.39%), followed by type II1 (19.4%), type III1 (16.1%), and type III2 (12.9%). Type I2 was occasionally observed (Table 3; Figure 6A).

The northeastern area: Four types of pore throat structures developed: type II1 was the most common (37.5%), followed by type II2 (31.3%), type I2 (18.8%), and type III1 (12.5%) (Table 3; Figure 6B).

The eastern area: three types of pore structures have developed: type II1 was the most developed (40.9%), followed by Type I1 (31.8%) and Type II2 (27.3%) (Table 3; Figure 6C).

4.5 Porosity and permeability

Physical analysis results were analyzed according to the Chinese reservoir classification standard (SY/T6285-2011). Given that the permeability span of the UMoLGF is large, the median value was applied to evaluate the permeability. The results were as follows:

The northwestern area: porosity ranged from 3.4% to 28.1% (avg. 13.8%), mainly were low porosity (Figure 7A); Permeability varied from 0.04 to 85.8 mD (average: 4.75 mD, median: 1.0 mD), which were mainly ultra-low permeability (Figure 7B).

The northeastern area: porosity varied between 2.0% and 27.1% (avg. 14.3%), dominated by low porosity (Figure 7C). The permeability span was relatively large, ranging from 0.02 to 89.5 mD (average: 4.97 mD, median: 0.57 mD) and dominated by ultra-low permeability (Figure 7D).

The eastern area: porosity ranged from 0.5% to 25.0% (avg. 8.7%), and was dominated by extra-low

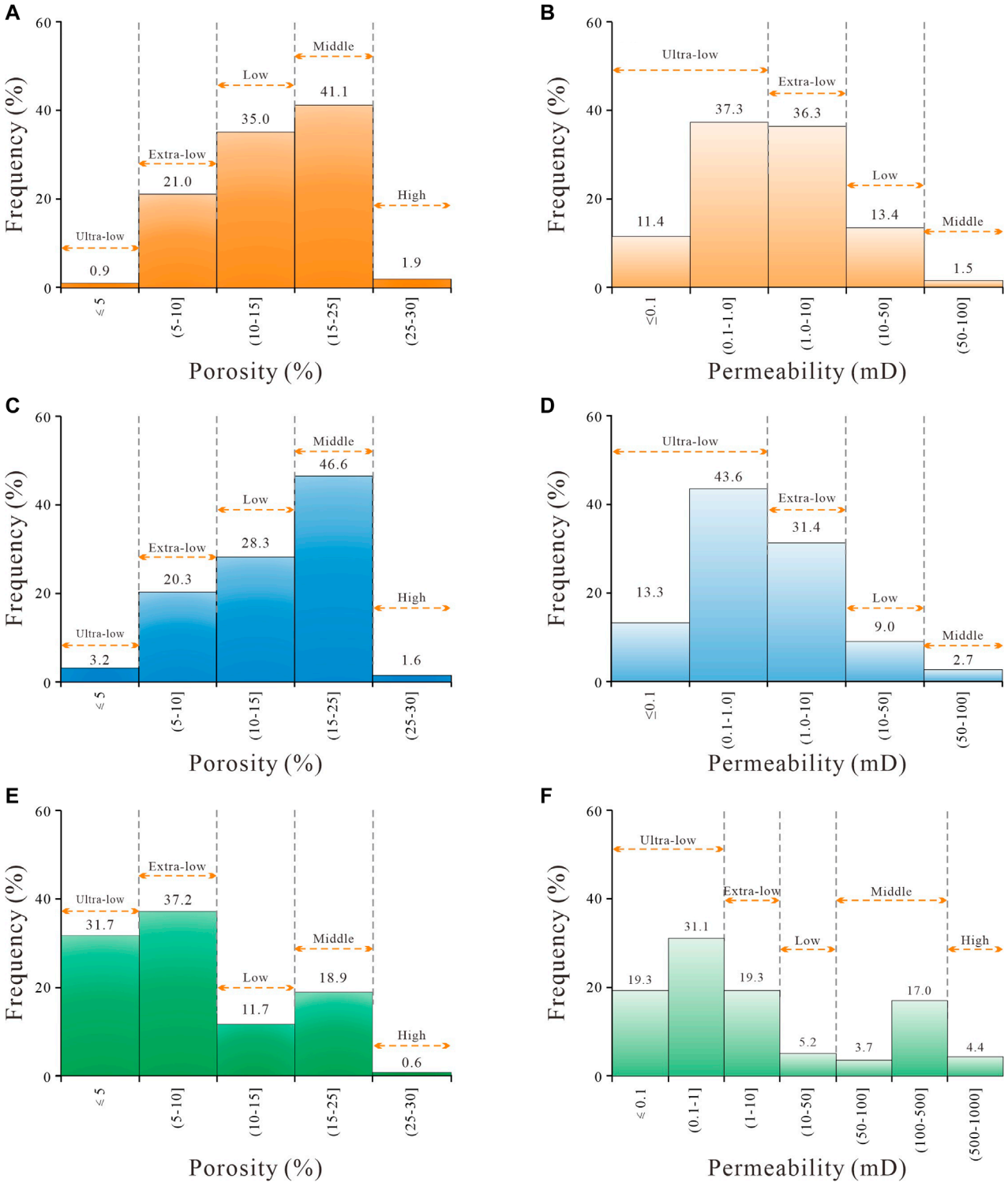

FIGURE 7
Distribution histogram of porosity in the **(A)** northwestern, **(C)** northeastern, and **(E)** eastern areas. Permeability in the **(B)** northwestern, **(D)** northeastern, and **(F)** eastern areas.

porosity (Figure 7E). The permeability span was large, varies from 0.02 to 826.9 mD (average: 74.7 mD, median: 0.85 mD) and dominated by ultra-low permeability (Figure 7F).

Overall, the UMoLGF is an ultra-low permeability reservoir, with varying porosity across different areas. The reservoir properties in the northwestern and northeastern areas were similar, While, the eastern area generally has relatively superior permeability.

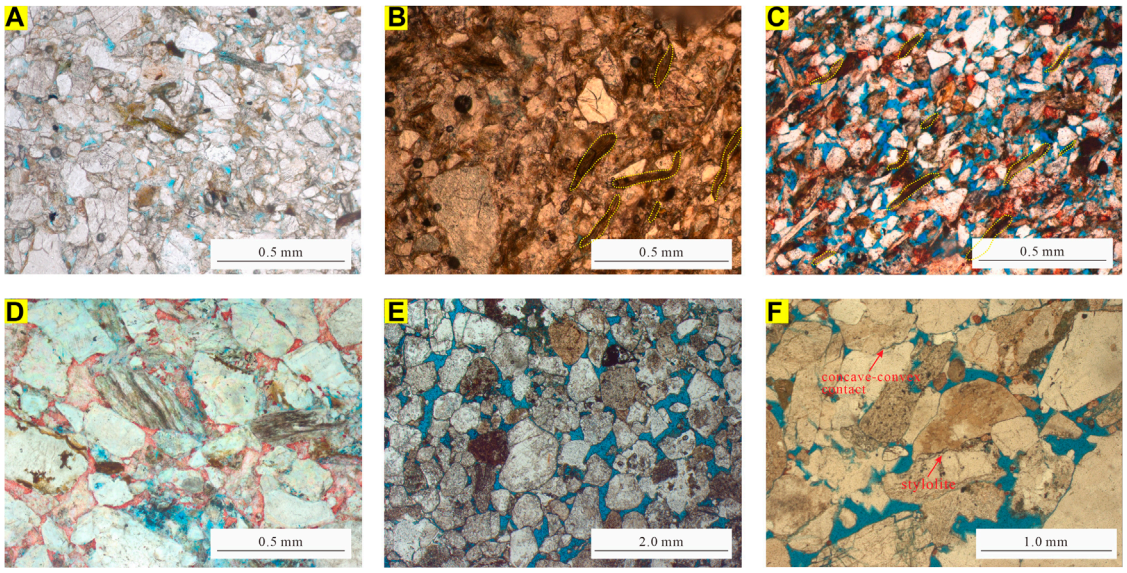

FIGURE 8
Compaction characteristics of the study areas in the UMoLGF: **(A)** N104, 1340.29 m, particles in point and line contact; **(B)** N5, 781.08 m, particles floating, directional arrangement of mica; **(C)** L87, 1411.35 m, particles in point contact, directional arrangement of mica; **(D)** L96, 804.07 m, particles in point contact; **(E)** MB15, 1456.78 m, particles in point contact; **(F)** XX1, 4213.42 m, particles in concave-convex contact, stylolite line.

TABLE 4 Contact relationship between particles in different areas of the UMoLGF.

Area	Sample number	Pore types					Frequency (%)				
		Float	Point	Line	Point - line	Concave - convex	Float	Point	Line	Point - line	Concave - convex
The northwestern area	65	7	54	4	-	-	10.77	83.08	6.15	-	-
The northeastern area	71	10	54	7	-	-	14.08	76.06	9.86	-	-
The eastern area	58	5	40	3	5	5	8.62	68.97	5.17	8.62	8.62

4.6 Diagenesis

Combined the observation of CTS, SEM, and XRD, compaction, cementation, and dissolution were the main diagenetic events of the UMoLGF.

4.6.1 Compaction

The UMoLGF in the northwestern, northeastern, and eastern areas had medium–shallow burial. The following compactions can be observed under the microscope: (a) particles in the northwest, northeast, and east were mainly point contact (Figures 8A,C,D), accounting for 83.1%, 73.6%, and 69.0% (Table 4), respectively, followed by floating contacts (Figure 8B), accounting for 10.8%, 14.1%, and 8.6% (Table 4), respectively; (b) mica orientations were observed in the northwestern and northeastern areas (Figures 8B,C), and not in the eastern area (Table 4); (c) a small number of point-line contact (5.2%), line contact (8.6%), and concave-convex contact (8.6%) were observed in the eastern area (Table 4; Figures 8E,F). Stylolite was present in the eastern area (Figure 8F) but absent in the northwestern and northeastern areas (Table 4). Overall, the compaction intensity of the UMoLGF was weak.

4.6.2 Cementation

The cementation types of UMoLGF include carbonate, clay mineral, and siliceous cementation.

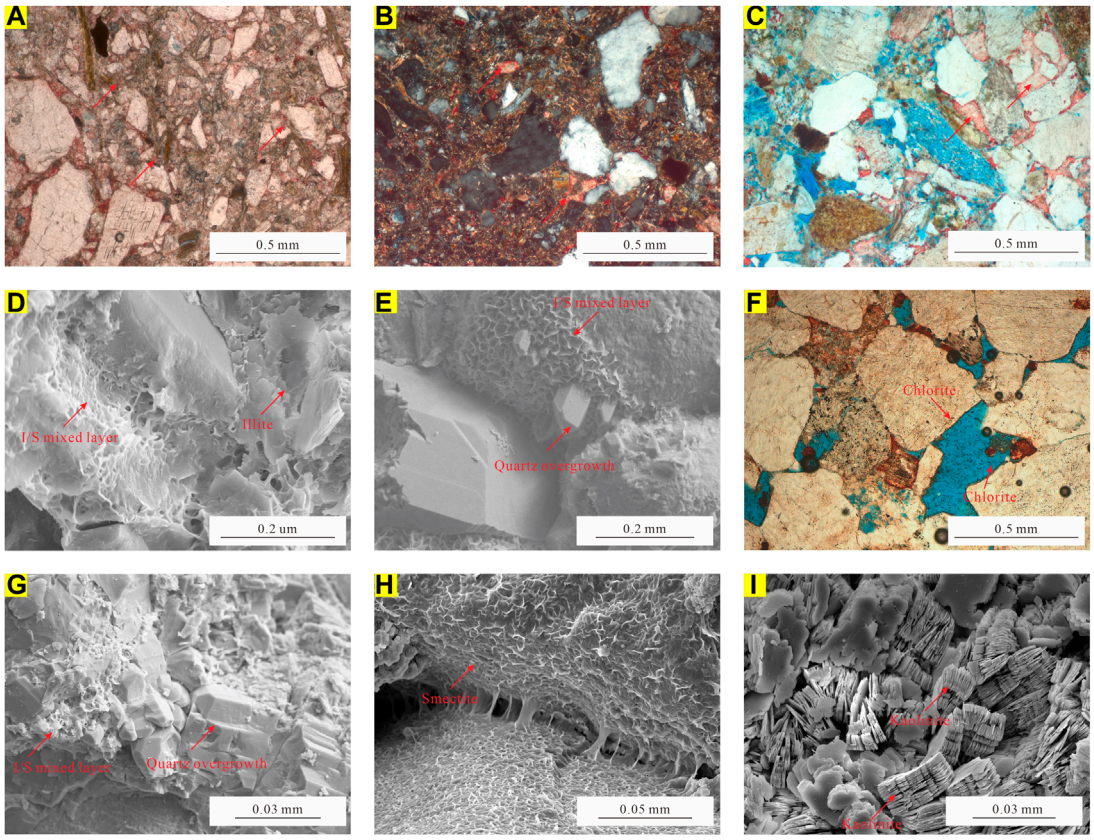

FIGURE 9
Cementation characteristics of the UMoLGF: **(A)** N5, 780.9 m, the first stage of calcite; **(B)** L96, 993.8 m, the first stage of calcite; **(C)** L96, 1006.5 m, the second stage of calcite; **(D)** L95, 824.8 m, illite and I/S mixed layer filled the intergranular pores; **(E)** XX1, 4213.2 m, the quartz overgrowth, the I/S mixed layer; **(F)** XX1, 4111.75 m, chlorite grows perpendicular to the surface of particles in a needle-like shape; **(G)** XX1, 4115.3 m, quartz overgrowth and I/S mixed layer; **(H)** MX101, 834.6 m, smectite exists in a thin film; **(I)** MX101, 831.4 m, kaolinite in a page form.

4.6.3 Carbonate cementation

Calcite was the most critical carbonate cement in the UMoLGF and was present in more than 85% of the samples. The calcite content in the northwestern and northeastern areas was relatively high, with an average of 8.20% and 7.50%, respectively; however, it was relatively low in the eastern area (avg. 5.70%).

Two stages of calcite developed in the UMoLGF: (a) during the early stage of diagenesis, particles floated, and the compaction intensity was weak. Calcite cement precipitated at the edges of the particles or filled the intergranular pores as small particles. The content of this kind of calcite was low (Figures 9A,B). (b) in the meso-diagenesis stage, calcite crystals precipitated among the skeleton particles, and its content was slightly higher than the first stage of calcite (Figure 9C).

4.6.4 Clay mineral cementation

Various clay minerals have been developed in the UMoLGF, including smectite, illite/smectite mixed layer (I/S mixed layer), chlorite, illite, and kaolinite. The clay mineral contents in different areas differed slightly. The I/S mixed layer (32.4% and 22.5%, respectively) and illite (30.1% and 31.9%, respectively) dominated the northwestern and northeastern areas, whereas illite (48.9%) and chlorite (27.8%) dominated the eastern area.

4.6.5 Smectite

The XRD results showed that smectite mainly existed in the northwestern, followed by the northeastern area, with minimal content in the east. According to the SEM observations, smectite typically wrapped mineral particles in a honeycomb-like and reticular aggregate, existing as a pore liner (Figure 9H).

4.6.6 I/S mixed layer

The I/S mixed layer mainly existed in honeycomb form (Figures 9D, E, G) and was widely developed in all three areas, with high content in the northwestern and northeastern areas.

4.6.7 Illite

Illite typically appeared as flakes and filaments. Illite aggregates were largely developed on particle as flakes (Figure 9D). Illite was the most important clay mineral in the three areas, with the highest content in the eastern area and similar contents in the northwestern and northeastern areas.

4.6.8 Chlorite

Chlorite was the most important clay mineral in the eastern area and less abundant in the northwestern and northeastern areas.

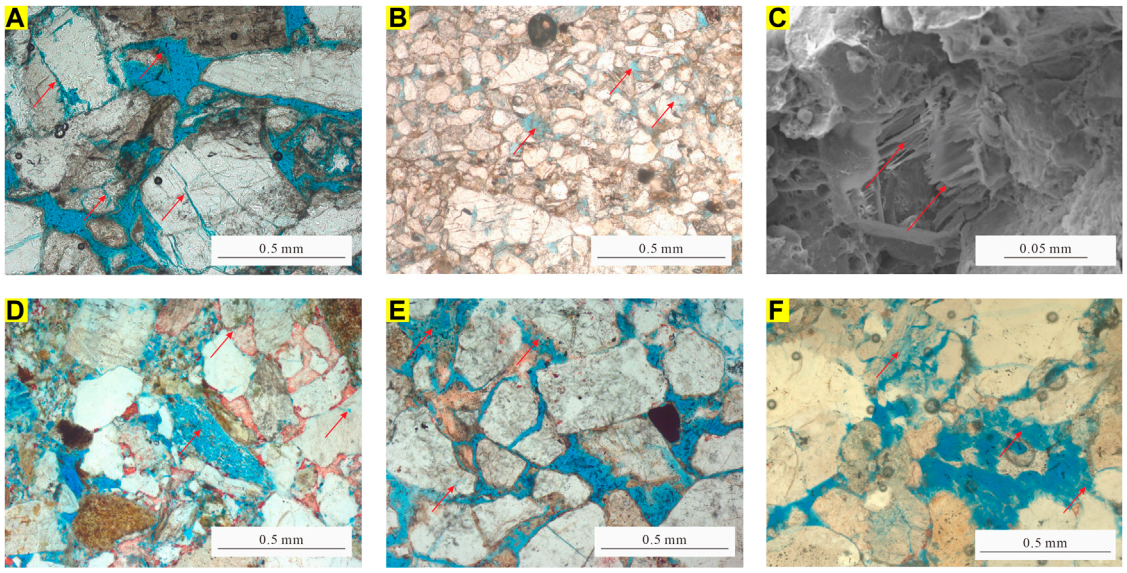

FIGURE 10
Dissolution characteristics of the study areas within the UMoLGF, **(A)** N3, 990.7 m, intergranular and intragranular dissolution pores, dissolution occurred along with feldspar cleavage fracture; **(B)** N104, 1636.48 m, the intergranular and intragranular dissolution pores; **(C)** Y2, 1422.5 m, dissolution occurred in the feldspar; **(D)** L96, 827.8 m, dissolution occurred in the feldspar, rock fragments, and calcite cement; **(E)** MB15, 1453.73 m, RIP and intergranular and intragranular dissolution pores; **(F)** XX1, 4208.16 m, intergranular and intragranular dissolution pores.

Chlorite typically grew perpendicular to the particle surface in a needle-like shape and existed as a pore lining (Figure 9F).

4.6.9 Kaolinite

The kaolinite content was low in all three areas. Thin section observations showed that only a small number of the samples developed page-like kaolinite (Figure 9I).

4.6.10 Quartz overgrowth

Siliceous cementation in the UMoLGF was relatively limited, characterized by quartz overgrowth (Figures 9E,G). The siliceous cementation content in the three areas was in the order of eastern > northwestern > northeastern, the overall content was low.

4.6.11 Dissolution

Dissolution is a critical diagenetic event in the UMoLGF, that can significantly improve reservoir properties in the northwestern and northeastern areas. Under a microscope, various dissolution phenomena can be observed. (a) Acidic fluids dissolved the interior of particles, forming intragranular dissolution pores in a spotted honeycomb shape (Figures 10A–F); (b) acidic fluid dissolved the cleavage fracture of feldspar, forming micro-fractures to enhance pore connectivity (Figure 10A); (c) intergranular dissolution pores formed owing to irregular dissolution at the edges of soluble particles (Figures 10A, B, D–F); (d) dissolution occurred in calcite cement, forming intragranular dissolution pores (Figures 10D,E). These dissolution phenomena were more prevalent in the northwestern and northeastern areas but scarce in the eastern area.

5 Discussion

5.1 Diagenetic stage

In this study, the diagenetic stages were divided based on the standard (SY/T5477-2003), and the basis for division was as follows.

a) Particles in the UMoLGF were mainly point contacts; b) Pores were mainly RIPs and secondary dissolution pores. The dissolution was dominated by feldspar dissolution, followed by rock fragment dissolution, and calcite dissolution; c) Ro is often used as a paleo-geothermal indicator of the organic matter and the basis for dividing the diagenesis stage. The Ro in the mudstone of the UMoLGF was between 0.47 and 0.53 (avg. 0.55); d) The distribution and morphology of authigenic minerals changed with formation temperature, pore fluid properties, and pressure. This formed different diagenetic minerals, corresponding to different diagenetic stages. The authigenic clay minerals of the UMoLGF were primarily illite, I/S mixed layer, and chlorite. The I/S mixed layer mostly developed on the grain surface in the form of a honeycomb; Illite predominately appeared as flakes. Chlorite grew on the surface as needle-like vertical particles and occasionally as rose-like particles. Smectite appeared as mesh and honeycomb-like particles. The kaolinite content was low, primarily appearing as book pages, and occasionally as worm-like particles. Two stages of calcite cementation were observed; quartz overgrowth was relatively rare and occasionally occurs in degrees of I-II.

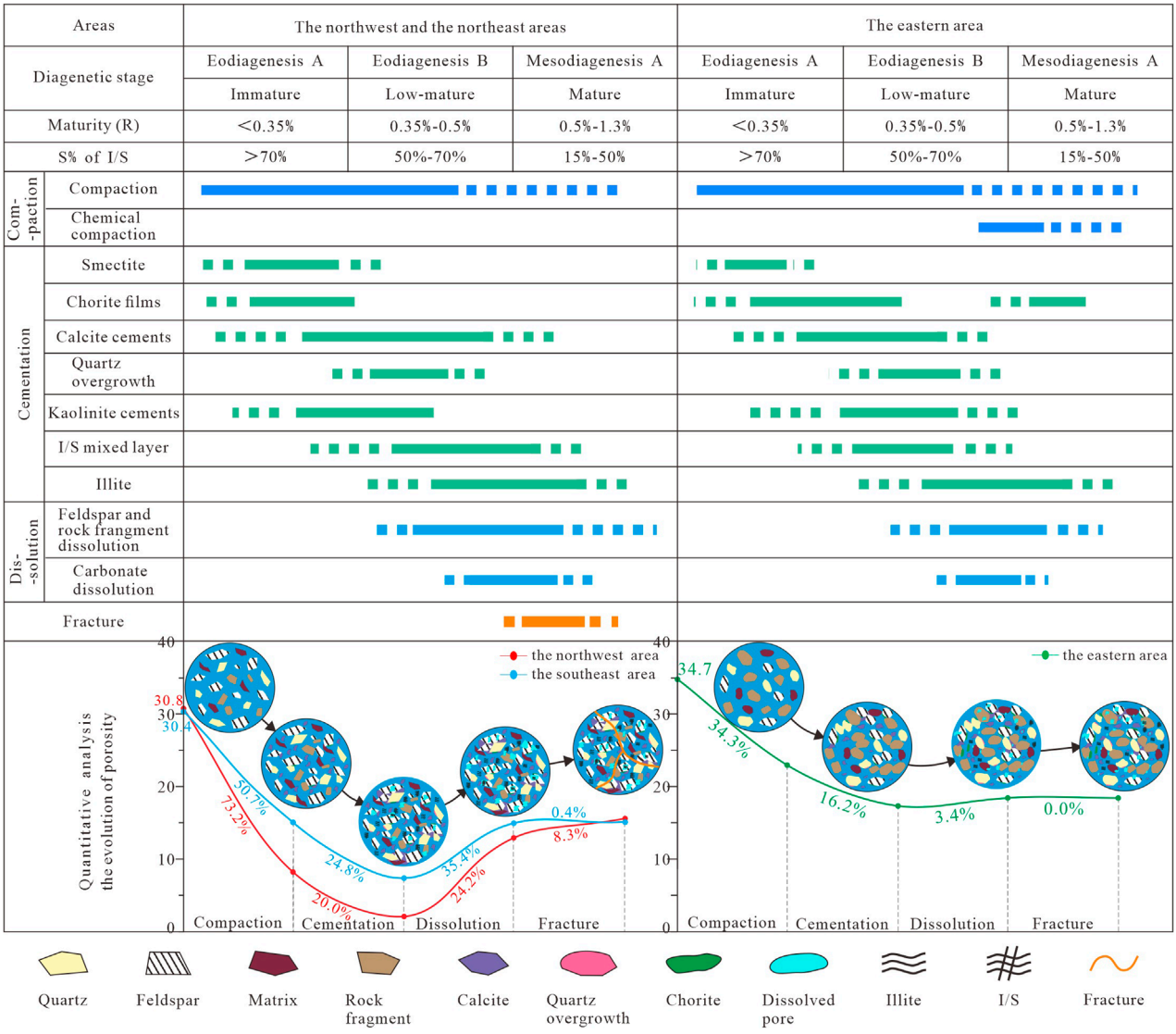

FIGURE 11
Porosity evolution models in different areas of the UMoLGF.

Accordingly, the UMoLGF in the study area has entered the eo-diagenesis B stage, with minor progression into the meso-diagenesis A stage (Figure 11).

5.2 Porosity evolution model

Pore evolution is affected by sedimentation and diagenesis (Liu et al., 2016; Zhou et al., 2017; Bai et al., 2021). Combined with the regional burial history, analytical test data, and porosity calculations (Table 5), this study established pore evolution models for the three areas (Figure 11).

Eo-diagenetic stage A: The intensity of cementation and dissolution was weak at the early burial stage. Compaction was the main diagenesis event in this stage, leading to a reduction in porosity in the three areas. At this stage, the particles floated with no contact between thm, while the RIPs dominated the reservoir space. The northwestern and northeastern areas were near-source deposits. The sediment transport distance was relatively short, resulting in poor sorting and roundness. However, these variables were superior in the eastern area owing to its far distance. Controlled by the influence of provenance, the initial porosities in the northwestern and northeastern areas were similarly (30.8% and 30.4%, respectively), while the eastern area had a high initial porosity (34.8%) (Table 5). The compaction intensity gradually increased with increased depth. At the end of this stage, particles were mainly in point contacts with few point-line contacts. Authigenic clay minerals, such as smectite and chlorite film, gradually precipitated, and calcite cement was observed (Figure 11).

TABLE 5 Quantitative calculation of porosity evolution in different areas of the UMoLGF.

Area	Core porosity P_{cor}/%	Initial porosity Φ_0/%	Porosity after compaction Φ_{com} (%)	Porosity after cementation Φ_{cem} (%)	Porosity after dissolution Φ_{dis} (%)	Porosity loss rate caused by compaction R_{com}/%	Porosity loss rate caused by cementation R_{cem}/%	Porosity loss rate caused by dissolution R_{dis}/%
The northwestern area	14.68	30.79	8.26	2.05	10.94	73.19	20.04	35.40
The northeastern area	13.95	30.44	15.03	7.48	7.50	50.66	24.82	24.17
The eastern area	17.82	34.75	22.98	17.32	1.17	34.30	16.19	3.43

Eo-diagenetic stage B: After entering this stage, the compaction intensity was further enhanced, ultimately peaking. Some mica was oriented in the northwestern and northeastern areas but not in the east. Quantitative calculations showed that the pore loss rates caused by compaction in the northwestern, northeastern, and eastern areas were 73.2%, 50.7%, and 34.3%, respectively (Table 5). The effect of dissolution on reservoir properties was gradually enhanced at this stage. Owing to the acidic fluid, the soluble substances were slightly corroded, forming secondary dissolution pores. Compared to the eastern area, the dissolution in the northwestern and northeastern areas was relatively strong. The influence of cementation on porosity was also enhanced at this stage. Crystalline calcite precipitated and filled the intergranular pores, and some kaolinite precipitated. Additionally, kaolinization of feldspar was observed in thin sections. Many illite and I/S mixed layers precipitated later in this stage. Cementation was relatively strong in the northwestern and northeastern areas. The dominant clay minerals in the northwestern and northeastern areas were I/S mixed layer and illite, while the eastern area was dominated by chlorite, illite, and I/S mixed layer (Figure 11). During this stage, cementation had the most significant influence on the reservoir. The porosity loss rate caused by cementation was relatively close in the northwestern (20.04%) and northeastern areas (24.82%), which was relatively low in the eastern area (16.19%) (Table 5).

Meso-diagenetic stage A: During this stage, the reservoir quality of the three areas was dominated by dissolution, with compaction and cementation having less impact. Chemical pressure dissolution occurred in the eastern area, and stylolite structure can be occasionally observed. This phenomenon was not detected in the northwestern or northeastern areas (Figure 11). Meanwhile, organic acids were continuously released during the thermal maturation of organic matter, and soluble substances dissolved towing to acidic fluids, forming secondary dissolution pores. Dissolution significantly improved reservoir properties in the northwestern and northeastern areas with weak effects in the eastern area. After dissolution, the porosities in the northwestern, northeastern, and eastern increased by 35.40%, 24.17%, and 3.43%, respectively (Table 5). Fractures were present in the northwestern and northeastern areas and not in the east (Figure 11).

5.3 Controlling factors of reservoir quality

5.3.1 Initial material

5.3.1.1 Grain size and sorting

Different provenance systems determined the differences in the initial material composition of the three areas. Grain size and sorting were foundational factors in determining the reservoir quality.

Owing to the short sediment transport distance, the northwestern and northeastern areas exhibited poor sorting and a relatively large median grain sizes. The sediment transport distance was long as the eastern area was located futher from the provenance. The water system in the eastern area was one of the most significant in the Paleogene of the Qaidam Basin, providing abundant energy. Hence, the sandstone in the eastern area was relatively well sorted, with a relatively small median grain size.

The median grain size showed a weak positive correlation with porosity (R^2 = 0.14, 0.13, 0.05, respectively) (Figure 12A) and permeability (R^2 = 0.33, 0.31, 0, respectively) (Figure 12B) in the northwestern, northeastern, and eastern areas. The reservoir properties of the three areas were weakly influenced by grain size. The sorting in the eastern area exhibited a significant negative correlation between porosity (R^2 = 0.67) (Figure 13A) and permeability (R^2 = 0.53) (Figure 13B). Meanwhile, the sorting in the northwestern and northeastern areas showed a weak correlation with porosity (R^2 = 0.01 and 0.09) (Figure 13A) and permeability (R^2 = 0.03 and 0.14) (Figure 13B). Overall, the initial material significantly influenced reservoir quality in the eastern area compared to the northwestern and northeastern areas.

5.3.1.2 Mud content

The mud content in the eastern area was substantially lower than that in the northwestern and northeastern areas. Given the hydrodynamic conditions in the eastern area, particles were fully elutriated during transportation, helping to preserve primary pores.

Mud content can greatly affect the reservoir properties. Under the overlying formation pressure, mud can directly fill the intergranular pores, reducing reservoir space and pore connectivity. Compared to the other areas, the northwestern area was significantly affected by mud content, with the effect on permeability (R^2 = 0.39)

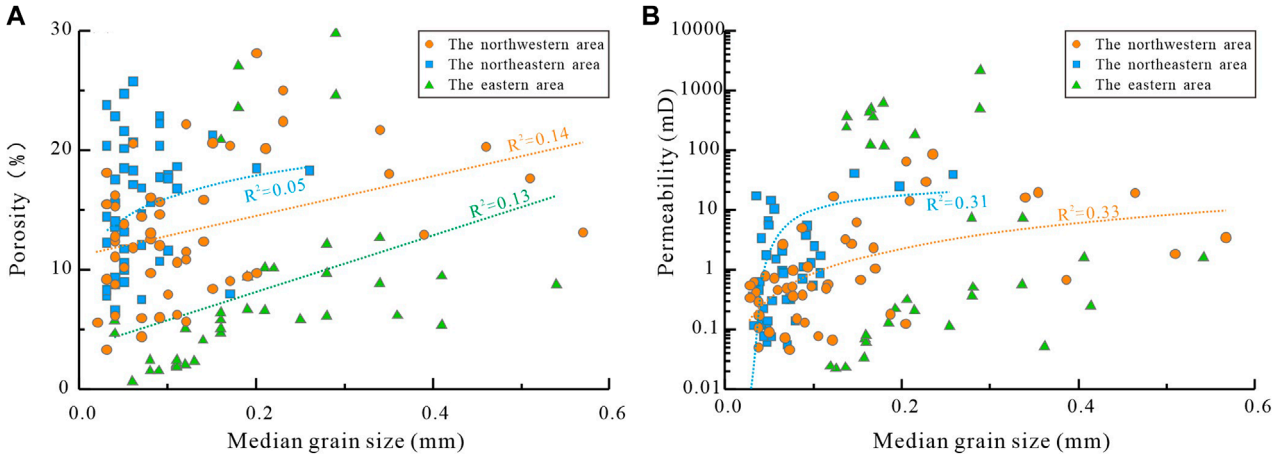

FIGURE 12
Relationship between the median grain size and **(A)** porosity and **(B)** permeability in different areas.

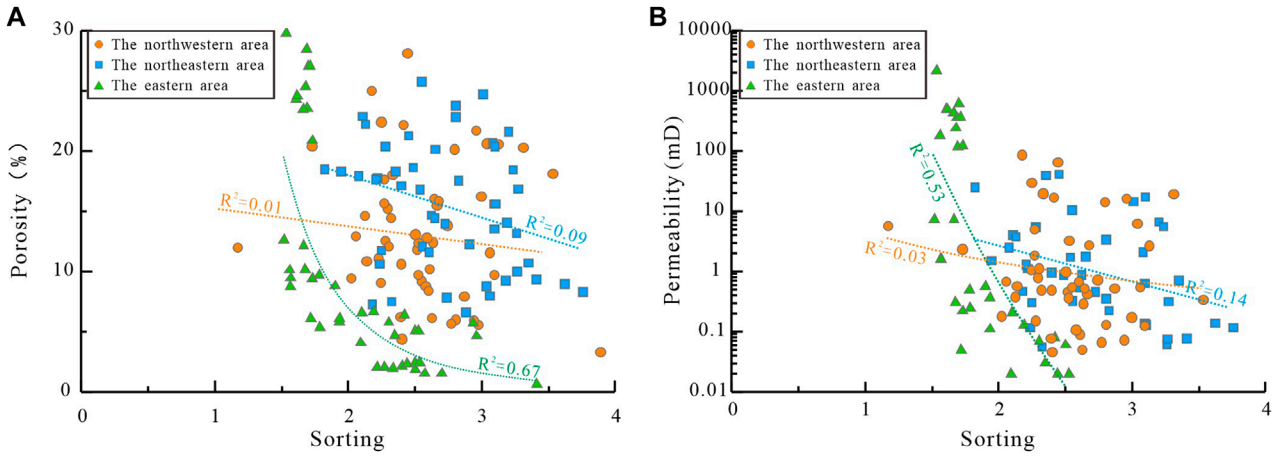

FIGURE 13
The cross-plots between the sorting and **(A)** porosity and **(B)** permeability in different areas.

greater than on porosity (R^2 = 0.11) (Figure 14). The mud content had minimal impact on the reservoir quality in the northeastern area and relatively no impact on the eastern area (Figure 14).

5.3.2 Diagenesis

Diagenesis significantly affects sandstone reservoirs quality, which can determine the preservation of primary and formation of secondary pores (Dou et al., 2023; Zhang et al., 2023). Owing to the differences in initial material composition, diagenesis can have varying impacts on reservoir quality.

5.3.2.1 Compaction

The UMoLGF burial depth was shallow, and the compaction was weak, significantly impacting the reservoir properties in all three areas. According to Houseknecht's (1989) relationship between intergranular pore volume and cement content, compaction was the primary cause of reservoir deterioration in all three areas. Compaction had the most significant impact on the northwestern area, followed by the northeastern area and eastern areas (Figure 15). The porosity loss rates owing to compaction significantly differed in the northwestern (73.19%), northeastern (50.66%), and eastern (34.30%) areas (Table 5).

5.3.2.2 Cementation

1) Carbonate cementation

Carbonate cementation can positively and negatively impact reservoir properties (Mansurbeg et al., 2008; Bjorlykke and Jahren, 2012; Zhang et al., 2015; Lai et al., 2018; Chen et al., 2019). It can directly fill the pores, reducing the reservoir properties. Alternatively, carbonate cement formed early can improve compaction resistance and protect primary pores. When subjected to acidic fluids, some carbonate cement dissolves and creates secondary pores, improving reservoir properties.

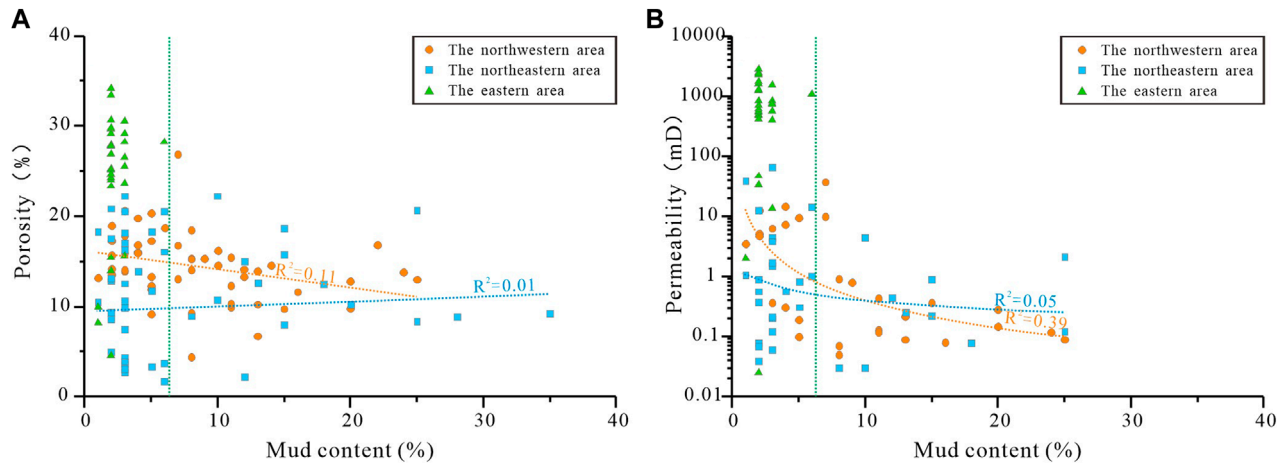

FIGURE 14
The cross-plots of the mud content and **(A)** porosity and **(B)** permeability in different areas.

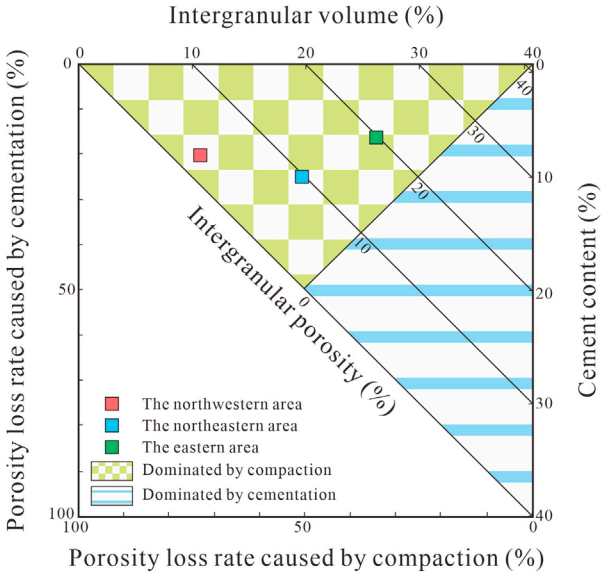

FIGURE 15
Influence of compaction and cementation on porosity of the UMoLGF in different areas.

Carbonate cement was dominated by calcite cement in the UMoLGF. The calcite contents in the northwestern and northeastern areas were high (average: 7.60% and 8.10%, respectively), Whereas that in the eastern area was relatively low (avg. 5.70%). The influence of calcite content on reservoir properties differed among the three areas.

The northwest area: The relationship between calcite content and reservoir properties is complex. When the calcite content was ≤10%, the porosity and permeability decreased as it increased (Supplementary Figure S1A, B). However, when the calcite content was between 10% and 20%, the porosity and permeability increased as it increased (Supplementary Figure S1A, B). Conversely, if the calcite content exceeded 20%, both porosity and permeability decreased as it increased (Supplementary Figure S1A, B). This can be explained as follows.

In the early stage of diagenesis, the calcite content was relatively low, mainly filling the primary pores and occupying some reservoir space. At this stage, compaction dominated diagenesis, while cementation and dissolution were relatively weak. The calcite content increased as cementation progressed, and the damage to reservoir properties gradually increased. The calcite content showed a negative correlation with reservoir properties in the early stages. Over time, dissolution gradually increased with diagenesis and the continuous release of organic acids, primarily from the maturation of organic matter. During this period, some calcite particles dissolved, creating small secondary dissolution pores and improving reservoir properties. Consequently, the reservoir properties improved with increasing calcite content. However, when the it exceeded 20%, the pores created by calcite dissolution were insufficient to offset the pores occupied by calcite filling. Therefore, the reservoir properties deteriorated with increasing calcite content.

The northeastern area: Compared to the northwestern area, the dissolution in this area was relatively weak. When the calcite content was less than 18%, it negatively correlated with porosity (R^2 = 0.23) and permeability (R^2 = 0.24) (Supplementary Figure S1C, D). When the calcite content was greater than 18%, both porosity and permeability showed a slight increase with the increase of it (Supplementary Figure S1C, D).

The reasons for this were as follows: In the early stage, some calcite precipitated, and dissolution was weak. At this time, the calcite content was low and largely existed in the pores. As the calcite content increased, the reservoir properties gradually deteriorated. As diagenesis progressed, dissolution gradually increased, and calcite dissolved to form some secondary pores, improving the reservoir properties.

The eastern area: The calcite content was low, and negatively correlated with porosity (R^2 = 0.50) (Supplementary Figure S1E) and permeability (R^2 = 0.56) (Supplementary Figure S1F). Calcite cements mainly developed in intergranular pores and occupied

a certain reservoir space, reducing reservoir properties. (2) Clay Mineral Cementation.

Clay mineral cementation is a crucial factor affecting reservoir properties. Reservoir properties were negatively correlated with clay mineral content in the study area. High clay mineral content was often associated with low porosity and permeability. Hence, the eastern area was significantly impacted by clay minerals compared to the northwestern and northeastern areas (Supplementary Figure S2).

The clay mineral content varied across different areas. Based on XRD results, the primary clay minerals in the northwestern and northeastern areas were the I/S mixed layer and illite. In contrast, illite and chlorite dominated the clay minerals in the eastern area.

Northwestern and Northeastern areas: The I/S mixed layer (honeycomb shape) and illite (filamentous or curved sheet shape) tended to fill the intergranular pores and occupy some reservoir space. They can also segment the reservoir space, making the initially narrow throat more tortuous and reducing pore connectivity. The cross-plots of the I/S mixed layer, illite, and reservoir properties revealed a destructive effect on reservoir properties, with illite having a relatively larger influence (Supplementary Figure S3). However, the overall impact was weak. The northeastern area was slightly affected by illite, and its effect on the porosity was more significant than on permeability (Supplementary Figure S3).

Eastern area: Filamentous illite filled the intergranular pores in the eastern area with a well-developed crystal morphology. Illite negatively correlated with porosity (R^2 = 0.45) and permeability (R^2 = 0.49) (Supplementary Figure S4), and exhibited a destructive effect on reservoir quality. Chlorite was well-developed in the eastern area, growing perpendicular to the particle surface in a pore-lining form, protecting the primary pores. The cross-plot of the chlorite content and reservoir properties showed that chlorite was positively correlated with porosity (R^2 = 0.26) and permeability (R^2 = 0.26) (Supplementary Figure S4).

5.3.2.3 Dissolution

Dissolution plays a crucial role in improving the reservoir quality. Secondary dissolution pores were positively correlated with porosity (R^2 = 0.24, 0.57, and 0.11, respectively) (Supplementary Figure S5A), permeability (R^2 = 0.28, 0.57, and 0.05, respectively) (Supplementary Figure S5B), and thin section porosity (R^2 = 0.92, 0.45, and 0.71, respectively) (Supplementary Figure S5C) in the northwestern, northeastern. And eastern areas.

Quantitative calculation results reveal that dissolution affected the three areas differently. Dissolution in the northwestern area was the strongest, followed by the northeastern area and eastern areas. The porosity increase rates caused by dissolution were 35.40%, 24.17%, and 3.43%, respectively, for the northwestern, northeastern, and eastern areas. The main reasons are as follows. Dissolution is closely related to organic acids produced by source rocks, deep hydrothermal fluids, near-surface atmospheric freshwater leaching, and freshwater leaching under an unconformity surface. The Lower Jurassic reservoir, the source rock in the NMoQB, is widely developed in the northwestern and northeastern areas (Yao et al., 2017). When organic matter is converted to hydrocarbons, it releases a significant amount of CO_2 and produces carboxylic acids. The Lower Jurassic reservoir in the NMoQB contains coal-bearing source rocks, resulting in a higher concentration of organic acids compared with other source rocks. Organic acids can then be transported to the UMoLGF through faults or pores, increasing the acidity of pore fluids in the northwestern and northeastern areas, and ultimately promoting dissolution.

The petrological characteristics showed that the feldspar content in the northwestern and northeastern areas was relatively high, and the rock fragments in these areas were dominated by volcanic and metamorphic rock debris, respectively. In contrast, in the eastern area, the feldspar content was low, the debris was mainly metamorphic rock debris, and the soluble volcanic rock debris was low. Under the action of acidic fluids, unstable minerals easily dissolve and form secondary pores. Overall, the northwestern and northeastern areas had a more suitable material basis for dissolution than the eastern area.

Furthermore, the conversion of clay materials produces acidic fluids, which promote dissolution. For example, H^+ is produced when smectite is converted into illite, increasing the acidity of diagenetic fluids. Indeed, the XRD results indicate that smectite content is higher in the northwestern and northeastern than the eastern. Thus, compared with the eastern area, the northwestern and northeastern areas had better conditions for dissolution.

5.3.3 Fractures

Fractures were primarily developed in the northwestern area, accounting for 12.23% of the total thin section porosity (Table 2). The northwestern area features a sizable nose-shaped uplift with a piedmont tilt to the basin (Wu et al., 2016; Ren et al., 2019). Owing to frequent tectonic activity, multiple sets of fault systems have developed in this area, resulting in various fractures. The presence of fractures facilitated the migration of acidic fluids, thereby promoting dissolution.

According to CTS observations, samples with fractures generally had higher permeability than those without fractures in the northwestern area (Supplementary Figure S6A). However, fractures had little influence on core porosity (R^2 = 0.05) (Supplementary Figure S6B) and thin section porosity (R^2 =0.07) ((Supplementary Figure S6D), while positively correlating with core permeability (R^2 =0.46) ((Supplementary Figure S6C). Thus, fractures are essential for improving the permeability in this area.

Oil and gas can effectively migrate through micro-fractures with openings larger than 0.1 μm (Anders et al., 2014). Hence, given that the fracture opening in the northwestern area was 2.17–51.86 μm, the fractures could serve as a reservoir space and a dominant channel for oil and gas migration. This can significantly improve reservoir properties in the northwestern area.

5.4 Controlling factors of high-quality reservoir

According to the above analysis, reservoir quality of the UMoLGF is controlled by multiple factors such as provenance (e.g., sorting and mud content), diagenetic events, and fractures. However, high-quality reservoirs' formation mechanisms and controlling factors significantly differ among the study areas.

The northwestern area: The reservoir space is well-developed, mainly with secondary dissolution pores, followed by fractures and a few RIPs. Fan delta deposits developed in this area. Soluble substance content (e.g., feldspar and debris) was high, conducive to dissolution. The organic acids produced in the Lower Jurassic source rocks further enhanced dissolution. Addtionally, this area has a large, nose-shaped uplift with a high northwest and a low southeast direction. The frequent tectonic activity in this area has led to multiple sets of fault systems. The associated fractures provide reservoir space and act as channels for hydrocarbon migration. Hence, in this area, the development of high-quality reservoirs relied on strong dissolution and widely developed fractures.

The northeast area: Pores were mainly secondary dissolution pores, followed by RIPs. This area also developed a fan delta sedimentary system. Compared to that in the northwestern area, reservoirs in this area have the following advantages: (a) the scale of sand deposits is more extensive and their distribution is wider; (b) sandstone particle sorting and pore structure are superior; (c) cementation is weaker; and (d) the soluble particle content is higher, and the Lower Jurassic source rocks providing organic acids. Thus, this area has favorable conditions for dissolution. In summary, the essential factors determining the high-quality reservoir include a favorable sedimentary environment that ensures the extensive distribution of sand bodies, and favorable dissolution leading to secondary dissolution pores.

The eastern area: RIPs and secondary dissolution pores dominated the reservoir space. The eastern area developed a braided river delta. Compared with those in the northwestern and northeastern areas, the eastern area has a better material basis: (a) the sorting of sandstone particles is good; (b) mud content is lower; (c) the sand body size is larger and its distribution is wider; and (d) pore structure is good. Regarding diagenetic transformation, compaction and cementation have little impact on reservoir properties in this area. Dissolution can create some secondary pores, and chlorite, which can protect RIPs, is widely developed in this area. Overall, the formation of high-quality reservoirs in this area depends on a favorable material basis, chlorite cementation, and dissolution.

6 Conclusion

1) Three provenance systems developed in the study area: northwest, northeast, and east. The northwestern and northeastern areas have similar reservoir characteristics with feldspar as the dominant rock type. Secondary dissolution pores dominate pore types. However, the northwestern area had more developed fractures and poorer pore structures compared to the northeastern area. In contrast, the eastern area contained a high rock fragment, with feldspathic litharenite and lithic arkose as the primary rock types. Furthermore, the sorting and roundness are superior and RIPs are the predominant pore type with a suitable pore structure.
2) UMoLGF has entered the eo-diagenesis B stage, with minor progression into the meso-diagenesis A stage. The pore evolution models in the northwestern and eastern areas were similar, whereas those in the eastern area slightly differed. The initial porosities in the northwestern, northeastern, and eastern areas were 30.8%, 30.4%, and 34.8%, respectively. Compaction significantly influenced the northwestern area. The porosity loss rates caused by compaction in the northwest, northeast, and eastern regions are 73.2%, 50.7%, and 34.3%, respectively. Cementation significantly affected the northwestern and northeastern areas, resulting in 20.0% and 24.8% porosity loss rates, respectively. In contrast, its impact on the eastern area was relatively small, with a porosity loss rate of 16.2%. Dissolution was essential for improving reservoir properties; the increased porosity rates owing to dissolution in the northwestern, northeastern, and eastern areas were 35.4%, 24.2%, and 3.4%, respectively.
3) The factors controlling high-quality reservoirs formation in the low-permeability UMoLGF differed among study areas. Compaction was the primary cause of porosity deterioration in all three areas. Strong dissolution and widely developed fractures significantly affected the northwestern high-quality reservoirs. Meanwhile, the northeastern area was dominated by provenance and diagenesis. The provenance provided a suitable material basis and favorable dissolution conditions can further improve reservoir quality. The eastern area was less affected by diagenesis; however, its provenance provided a good material basis. The sorting, rounding, pore type, and pore-throat structures were good. Dissolution and chlorite cementation can improve its reservoir properties.

Data availability statement

The original contributions presented in the study are included in the article/Supplementary Material, further inquiries can be directed to the corresponding author.

Author contributions

WL: Software, Writing–review and editing, Writing–original draft, Visualization, Validation, Project administration, Methodology, Investigation, Formal Analysis, Data curation, Conceptualization. DH: Writing–review and editing, Writing–original draft, Visualization, Supervision, Project administration, Methodology, Investigation, Funding acquisition, Formal Analysis, Conceptualization. CG: Writing–review and editing, Supervision, Project administration, Methodology, Formal Analysis, Conceptualization. TF: Writing–review and editing, Supervision, Project administration, Formal Analysis, Conceptualization. YC: Writing–review and editing, Visualization, Investigation, Funding acquisition, Data curation. Ya'L: Software, Writing–review and editing, Validation, Resources, Investigation, Funding acquisition. QS: Software, Writing–review and editing, Validation, Resources, Investigation, Funding acquisition. QL: Writing–review and editing, Software, Investigation, Data curation.

Funding

The author(s) declare that financial support was received for the research, authorship, and/or publication of this article. This study was jointly funded by the project from the Research Institute of Exploration and Development of Qinghai Oilfield (Grant 2018-Technique-Exploration-02) and the PetroChina prospective basic strategic technology research project (Grant 2022DJ3209).

Acknowledgments

We sincerely thank the Research Institute of Exploration and Development of Qinghai Oilfield Company, PetroChina, for generously providing us with research data and samples. Additionally, we are grateful to the journal editor and reviewers for their valuable comments and suggestions that significantly improved the quality of this manuscript.

Conflict of interest

Authors WL, DH, YC, and QL were employed by PetroChina. Author CG was employed by China National Oil and Gas Exploration and Development Company Ltd. Authors Ya'L and QS were employed by Research Institute of Exploration and Development of Qinghai Oilfield Company, PetroChina.

The remaining author declares that the research was conducted in the absence of any commercial or financial relationships that could be construed as a potential conflict of interest..

Publisher's note

All claims expressed in this article are solely those of the authors and do not necessarily represent those of their affiliated organizations, or those of the publisher, the editors and the reviewers. Any product that may be evaluated in this article, or claim that may be made by its manufacturer, is not guaranteed or endorsed by the publisher.

Supplementary material

The Supplementary Material for this article can be found online at: https://www.frontiersin.org/articles/10.3389/feart.2024.1396061/full#supplementary-material

References

Anders, M. H., Laubach, S. E., and Scholz, C. H. (2014). Microfractures: a review. *J. Struct. Geol.* 69, 377–394. doi:10.1016/j.jsg.2014.05.011

Bai, R., Wu, C. Y., Du, W., Geng, D., and Li, W. (2021). Characteristics and controlling factors of tight sandstone reservoirs: a case study of the Triassic Chang 7 and Chang 10 reservoirs in the Shanbei area, Ordos Basin. *J. Northwest Univ. Nat. Sci. Ed.* 51 (1), 95–108. doi:10.16152/j.cnki.xdxbzr.2021-01-012

Beard, D. C., and Weyl, P. K. (1973). Influence of texture on porosity and permeability of unconsolidated sand. *AAPG Bull.* 57 (2), 349–369. doi:10.1306/819A4272-16C5-11D7-8645000102C1865D

Bhatia, M. R., and Crook, K. A. W. (1986). Trace element characteristics of graywackes and tectonic setting discrimination of sedimentary basins. *Contrib. Mineral. Petrol.* 92, 181–193. doi:10.1007/BF00375292

Bjørkum, P. A., Walderhaug, O., and Aase, N. E. (1993). A model for the effect of illitization on porosity and quartz cementation of sandstones. *J. Sediment. Petrol.* 63 (6), 1089–1091. doi:10.2110/jsr.63.1089

Bjørlykke, K. (1993). Fluid flow in sedimentary basins. *Sediment. Geol.* 86 (1-2), 137–158. doi:10.1016/0037-0738(93)90137-T

Bjørlykke, K. (2014). Relationships between depositional environments, burial history and rock properties. Some principal aspects of diagenetic process in sedimentary basins. *Sediment. Geol.* 301, 1–14. doi:10.1016/j.sedgeo.2013.12.002

Bjorlykke, K., and Jahren, J. (2012). Open or closed geochemical systems during diagenesis in sedimentary basins: constraints on mass transfer during diagenesis and the prediction of porosity in sandstone and carbonate reservoirs. *AAPG Bull.* 96, 2193–2214. doi:10.1306/04301211139

Cao, B. F., Luo, X. R., Zhang, L. K., Sui, F. G., Lin, H. X., and Lei, Y. H. (2017). Diagenetic evolution of deep sandstones and multiple-stage oil entrapment: a case study from the Lower Jurassic Sangonghe Formation in the Fukang Sag, central Junggar Basin (NW China). *J. Pet. Sci. Eng.* 152, 136–155. doi:10.1016/j.petrol.2017.02.019

Cao, Y. C., Yang, T., Song, M. S., Wang, Y. Z., Ma, B. B., Wang, J., et al. (2018). Characteristics of low-permeability clastic reservoir sand genesis of relatively high-quality reservoirs in the continental rift lake basin: a case study of Paleogene in the Dongying sag, Jiyang depression. *Acta Pet. Sin.* 39 (7), 727–743. doi:10.7623/syxb/201807001

Chen, J., Shi, J. A., Long, G. H., Zhang, J., Wang, M., Zhou, F., et al. (2013). Sedimentary facies and models for the Palaeogene-Neogene deposits on the northern margin of the Qaidam Basin, Qinghai. *Sediment. Geol. Tethyan Geol.* 33, 16–26. doi:10.3969/j.issn.1009-3850.2013.03.003

Chen, J. F., Yao, J. L., Mao, Z. G., Li, Q., Luo, A. X., Deng, X. Q., et al. (2019). Sedimentary and diagenetic controls on reservoir quality of low-porosity and low-permeability sandstone reservoirs in Chang101, upper Triassic Yanchang Formation in the Shanbei area, Ordos Basin, China. *Mar. Pet. Geol.* 105, 204–221. doi:10.1016/j.marpetgeo.2019.04.027

Chen, Y. P., Liu, Z., Li, W. L., Dang, Y. Q., and Ma, D. D. (2008). Tectonic evolution and formation of reservoirs in Qaidam Basin. *J. Southwest. Petroleum Inst. Nat. Sci. Ed.* 29, 43–47. doi:10.3863/j.issn.1000-2634.2008.04.011

Cui, M. M., Li, J. B., Wang, Z. X., Fan, A. P., Gao, W. L., Li, Y. J., et al. (2019). Characteristics of tight sand reservoir and controlling factors of high-quality reservoir at braided delta front: a case study from Member 8 of Shihezi Formation in southwestern Sulige gas field. *Acta Pet. Sin.* 40 (3), 279–294. doi:10.7623/syxb201903003

Dou, W. C., Lin, M., Liu, L. F., and Jia, L. B. (2023). The effect of chlorite rims on reservoir quality in Chang 7 sandstone reservoirs in the Ordos Basin, China. *Mar. Pet. Geol.* 158, 106506. doi:10.1016/j.marpetgeo.2023.106506

Dutton, S. P., Loucks, R. G., and Day-Stirrat, R. J. (2012). Impact of regional variation in detrital mineral composition on reservoir quality in deep to ultradeep lower Miocene sandstones, western Gulf of Mexico. *Mar. Pet. Geol.* 35, 139–153. doi:10.1016/j.marpetgeo.2012.01.006

Feng, H. W., Xu, S. M., Wang, J. D., Zhang, G. L., Zeng, Z. P., and Shu, P. C. (2022). Jurassic provenances and their transition mechanism of the Delingha Sag in the eastern segment of northern margin of the Qaidam Basin, North Tibet. *Geosystems Geoenvironment* 1, 100097. doi:10.1016/j.geogeo.2022.100097

Fu, S. T. (2014). Natural gas exploration in Qaidam Basin. *China Pet. Explor.* 19, 1–10. doi:10.3969/j.issn.1672-7703.2014.04.001

Gao, Z. Y., Ma, J. Y., Cui, J. G., Feng, J. R., Zhou, C. M., and Wu, H. (2018). Deep reservoir pore evolution model of a geological process from burial compaction to lateral extrusion. *Acta Sedimentol. Sin.* 36, 176–187. doi:10.3969/j.issn.1000-0550.2018.019

Guan, P., and Jian, X. (2013). The cenozoic sedimentary record in Qaidam Basin and its implications for tectonic evolution of the northern Tibetan plateau. *Acta Sedimentol. Sin.* 31, 824–833. doi:10.14027/j.cnki.cjxb.2013.05.014

Guo, A. L., Zhang, G. W., Qiang, J., Sun, Y. G., Li, G., and Yao, A. P. (2009). Indosinian Zongwulong orogenic belt on the northeastern margin of the Tibetan Plateau. *Acta Petrol. Sin.* 25, 1–12. doi:10.00-0569/2009/025(01)-0001-12

Hu, W. R. (2009). The present and future of low permeability oil and gas in China. *Eng. Sci.* 11 (8), 29–37.

Hu, W. R., Wei, Y., and Bao, J. W. (2018). Development of the theory and technology for low permeability reservoirs in China. *Petroleum Explor. Dev.* 45 (4), 685–697. doi:10.1016/s1876-3804(18)30072-7

Huang, S. J., Wu, W. H., Liu, J., Shen, L. C., and Huang, C. G. (2003). Generation of secondary porosity by meteoric water during time of subaerial exposure: an example from yanchang formation sandstone of triassic of Ordos basin. *Earth Sci.* 28 (4), 419–424.

Ji, Y. L., Gao, C. L., Liu, Y. R., and Lu, H. (2015). Influence of hydrocarbon charging to the reservoir property in 1st member of funning formation in gaoyou depression. *J. Tongji Univ. Nat. Sci.* 43 (1), 133–139. doi:10.11908/j.issn.0253-374x.2015.01.020

Jia, Y. Y., Xing, X. J., Chen, J., Zhang, C. Y., Wang, Z., Shi, J. A., et al. (2014). The upper paleogene-lower neogene reservoir characteristics of nanbaxian Oilfield in the northern margin of Qaidam Basin. *J. Oil Gas Technol.* 36, 18–26.

Jian, X., Guan, P., Fu, L., Zhang, W., Shen, X. T., Fu, H. J., et al. (2024). Detrital zircon geochronology and provenance of Cenozoic deposits in the Qaidam basin, northern Tibetan plateau: an overview with new data, implications and perspectives. *Mar. Pet. Geol.* 159, 106566. doi:10.1016/j.marpetgeo.2023.106566

Jian, X., Guan, P., Zhang, W., Liang, H., Feng, F., and Fu, L. (2018). Late Cretaceous to early Eocene deformation in the northern Tibetan Plateau: detrital apatite fission track evidence from northern Qaidam basin. *Gondwana Res.* 60, 94–104. doi:10.1016/j.gr.2018.04.007

Jiang, Z. X., Li, F., Yang, H. J., Li, Z., Liu, L. F., Chen, L., et al. (2015). Development characteristics of fractures in Jurassic tight reservoir in Dibei area of Kuqa depression and its reservoir controlling mode. *Acta Pet. Sin.* 36 (S2), 102–111. doi:10.7623/syxb2015S2009

Karner, S. L., Chester, J. S., Chester, F. M., Kronenberg, A. K., and Hajash, A. (2005). Laboratory deformation of granular quartz sand: implications for the burial of clastic rocks. *AAPG Bull.* 89, 603–625. doi:10.1306/12200404010

Karner, S. L., Chester, J. S., Chester, F. M., Kronenberg, A. K., and Hajash, A. (2020). Characterization and impact on reservoir quality of fractures in the Cretaceous Qamchuqa Formation, Zagros folded belt. *Mar. Pet. Geol.* 113, 104117. doi:10.1016/j.marpetgeo.2019.104117

Lai, J., Wang, G. W., Wang, S., Cao, J. T., Li, M., Peng, X. J., et al. (2018). Review of diagenetic facies in tight sandstones: diagenesis, diagenetic minerals, and prediction via well logs. *Earth-Sci. Rev.* 185, 234–258. doi:10.1016/j.earscirev.2018.06.009

Li, F. J., Liu, Q., Liu, D. H., and Qi, W. Z. (2009). Characteristics and influential factors of low-ganchaigou formation reservoir in north edge of Qaidam Basin. *Nat. Gas. Geosci.* 20, 44–49.

Li, G. X., Shi, Y. J., Zhang, Y. S., Chen, Y., Zhang, G. Q., and Lei, T. (2022). New progress and enlightenment of oil and gas exploration and geological understanding in Qaidam Basin. *Litholigic Reserv.* 34, 1–18. doi:10.12108/yxyqc.20220601

Li, H., Tang, H. M., and Zheng, M. J. (2019a). Micropore structural heterogeneity of siliceous shale reservoir of the Longmaxi Formation in the southern Sichuan Basin, China. *Minerals* 9 (9), 548. doi:10.3390/min9090548

Li, S. E., Wang, D. H., Guan, P., Xiao, Y. J., Zhang, C., Hu, Q. T., et al. (2023). Difference and genesis of hydrocarbon-generation potential of Jurassic source rocks in different depressions in the eastern section of the northern margin of the Qaidam Basin. *Nat. Gas. Geosci.* 34, 1343–1356. doi:10.11764/j.issn.1672-1926.2023.04.002

Li, S. S., Peng, S., Chen, L., Li, S. Y., Li, L. Y., and Liu, X. Y. (2019b). A review on the complex reservoir sedimentary characteristics and low permeability formation of the upper eocene to lower oligocene in the wenchang B sag, pearl river estuary basin. *Geoscience* 33 (2), 357–369. doi:10.19657/j.geoscience.1000-8527.2019.02.11

Liu, J. K., Sun, Y. L., Jiao, X., and Zhang, Z. (2016). The genesis of low permeability of high-quality reservoirs in deep-buried clastic rock reservoir sand its development mechanism: a case study of Es2 Formation in the slope area of Qikou Sag. *Nat. Gas. Geosci.* 27 (5), 799–808.

Ma, X. M., Liu, C. Y., Luo, J. H., Chen, D. Y., and Zhang, J. K. (2016). Evolution history and hydrocarbon accumulation process of Late Cenozoic arcuate tectonic zone in the west section of the northern margin of Qaidam Basin. *Geol. Explor.* 52, 316–326. doi:10.13712/j.cnki.dzykt.2016.02.014

Maast, T. E., Jahren, J., and Bjorlykke, K. (2011). Diagenetic controls on reservoir quality in middle to upper jurassic sandstones in the south viking graben, north sea. *AAPG Bull.* 95 (11), 1937–1958. doi:10.1306/03071110122

Mansurbeg, H., Morad, S., Salem, A., Marfil, R., El-ghali, M. A. K., Nystuen, J. P., et al. (2008). Diagenesis and reservoir quality evolution of palaeocene deep-water, marine sandstones, the Shetland-Faroes Basin, British continental shelf. *Mar. Pet. Geol.* 25, 514–543. doi:10.1016/j.marpetgeo.2007.07.012

Morad, S., Ketzer, J. M., and De Ros, L. F. (2000). Spatial and temporal distribution of diagenetic alterations in siliciclastic rocks: implications for mass transfer in sedimentary basins. *Sedimentology* 47, 95–120. doi:10.1046/j.1365-3091.2000.00007.x

Pang, Y. M., Zou, K. Z., Guo, X. W., Chen, Y., Zhao, J., Zhou, F., et al. (2022). Geothermal regime and implications for basin resource exploration in the Qaidam Basin, northern Tibetan Plateau. *J. Asian Earth Sci.* 239, 105400. doi:10.1016/j.jseaes.2022.105400

Qin, S., Wang, R., Shi, W. Z., Geng, F., Luo, F. S., Li, G. P., et al. (2024). Integrated controls of tectonics, diagenesis and sedimentation on sandstone densification in the Cretaceous paleo-uplift settings, north Tarim Basin. *Geoenergy Sci. Eng.* 233, 212561. doi:10.1016/j.geoen.2023.212561

Qin, S., Wang, R., Shi, W. Z., Liu, K., Zhang, W., Xu, X. F., et al. (2022). Diverse effects of intragranular fractures on reservoir properties, diagenesis, and gas migration: insight from Permian tight sandstone in the Hangjinqi area, north Ordos Basin. *Mar. Pet. Geol.* 137, 105526. doi:10.1016/j.marpetgeo.2022.105526

Ren, C. Q., Gao, X. Z., Zhang, Y. S., Wang, B., Hou, Z. S., He, F. G., et al. (2019). Structural characteristics and hydrocarbon control action of paleogene/jurassic unconformity in Niudong area, North margin of Qaidam Basin. *Acta Geosci. Sin.* 40, 795–804. doi:10.3975/cagsb.2019.032801

Rossi, C., Kälin, O., Arribas, J., and Tortosa, A. (2002). Diagenesis, provenance, and reservoir quality of triassic TAGI sandstones from ourhoud field, berkine (ghadames) basin, Algeria. *Mar. Pet. Geol.* 19, 117–142. doi:10.1016/S0264-8172(02)00004-1

Samir, M. Z. (2013). Provenance, diagenesis, tectonic setting and reservoir quality of the sandstones of the Kareem Formation, Gulf of Suez, Egypt. *J. Afr. Earth Sci.* 85, 31–52. doi:10.1016/j.jafrearsci.2013.04.010

Shi, J. A., Wang, J. P., Mao, M. L., Wang, Q., Guo, Z. Q., Guo, X. L., et al. (2003). Reservoir sandstone diagenesis of memeber 6 to 8 in yanchang formation (triassic), xifeng Oilfield, Ordos basin. *Acta Sedimentol. Sin.* 21 (3), 373–380.

Su, J. L., Lin, L. B., Yu, Y., Wang, Z. K., and Li, Y. H. (2023). Comparative study on the provenance and reservoir characteristics of the second and fourth members of the upper triassic xujiahe formation in the xinchang area, western sichuan, China. *Acta Sedimentol. Sin.* 41, 1451–1467. doi:10.14027/j.issn.1000-0550.2022.142

Sun, B., Wang, J. D., Wang, D. H., Xiao, Y. J., Zhang, J. F., Chai, X. P., et al. (2019). Mesozoic-Cenozoic structural evolution and its control over oil and gas in the eastern section of the northern margin of the Qaidam Basin. *China Pet. Explor.* 24, 351–360. doi:10.3969/j.issn.1672-7703.2019.03.008

Sun, G. Q., Ma, J. Y., Wang, H. F., Chen, J., Zhang, Y. S., Jia, Y. Y., et al. (2012). Characteristics and significances of carbonate cements in northern Mahai region, northern margin of Qaidam Basin. *Petroleum Geol. Exp.* 34, 134–139.

Sun, G. Q., Zheng, J. J., Su, L., Liu, X. W., Yang, X., and Liu, Y. H. (2010). Mesozoic-cenozoic tectonic evolution in northwestern Qaidam Basin. *Nat. Gas. Geosci.* 21, 212–217.

Taylor, T. R., Giles, M. R., Hathon, L. A., Diggs, T. N., Braunsdorf, N. R., Birbiglia, G. V., et al. (2010). Sandstone diagenesis and reservoir quality prediction: models, myths, and reality. *AAPG Bull.* 94 (8), 1093–1132. doi:10.1306/04211009123

Tian, J. X., Ji, B. Q., Zeng, X., Wang, Y. T., Li, Y. L., and Sun, G. Q. (2022). Development characteristics and main control factors of deep clastic reservoir of Xiaganchaigou Formation in the northern margin of Qaidam Basin. *Nat. Gas. Geosci.* 33, 720–730. doi:10.1016/j.jnggs.2022.08.005

Tian, J. X., Li, J., Zeng, X., Kong, H., Sha, W., Guo, Z. Q., et al. (2020). Discovery and accumulation model of oil cracking gas reservoirs in Dongping area, Qaidam Basin. *Acta Pet. Sin.* 41, 154–162. doi:10.7623/syxb202002002

Wang, D. Y., Zheng, X. M., Li, F. J., Wang, F., Liu, Z. L., Wang, Z. K., et al. (2003). Forming condition of high-quality reservoir and its relative problems in low porosity and permeability enrichment zone. *Nat. Gas. Geosci.* 14 (2), 5. doi:10.3969/j.issn.1672-1926.2003.02.002

Wang, J., Cao, Y. C., Liu, K. Y., Liu, J., and Muhammad, K. (2017). Identification of sedimentary-diagenetic facies and reservoir porosity and permeability prediction: an example from the Eocene beach-bar sandstone in the Dongying Depression, China. *Mar. Pet. Geol.* 82, 69–84. doi:10.1016/j.marpetgeo.2017.02.004

Wang, Q. Q., Yuan, S. H., Wang, Y. D., Li, W. M., Liu, Y. J., Zheng, S. G., et al. (2023). The nature of the cenozoic western Qaidam Basin. *J. Jilin Univ. Earth Sci. Ed.* 53, 1–23. doi:10.13278/j.cnki.jjuese.20220224

Wang, R. F., Chi, Y. G., Zhang, L., He, H. H., Tang, Z. X., and Liu, Z. (2018). Comparative studies of microscopic pore throat characteristics of unconventional super-low permeability sandstone reservoirs: examples of Chang 6 and Chang 8 reservoirs of Yanchang Formation in Ordos Basin, China. *J. Petroleum Sci. Eng.* 160, 72–90. doi:10.1016/j.petrol.2017.10.030

Weltje, G. J., and Von Eynatten, H. (2004). Quantitative provenance analysis of sediments: review and outlook. *Sediment. Geol.* 171, 1–11. doi:10.1016/j.sedgeo.2004.05.007

Worden, R. H., Bukar, M., and Shell, P. (2018). The effect of oil emplacement on quartz cementation in a deeply buried sandstone reservoir. *AAPG Bull.* 102 (01), 49–75. doi:10.1306/02071716001

Wu, Y. Q., Tahmasebi, P., Lin, C. Y., Zahid, M. A., Dong, C. M., Golab, A. N., et al. (2019). A comprehensive study on geometric, topological and fractal characterizations of pore systems in low-permeability reservoirs based on SEM, MICP, NMR, and X-ray CT experiments. *Mar. Pet. Geol.* 103, 12–28. doi:10.1016/j.marpetgeo.2019.02.003

Wu, Z. X., Wang, B., Zhao, J., Zou, K. Z., Zhou, F., and Xiong, K. (2016). Diagenesis of Jurassic and its influence on reservoir properties in Niudong area, eastern Altun foreland. *Lithol. Reserv.* 28, 58–64. doi:10.3969/j.issn.1673-8926.2016.01.007

Xie, L., Xin, X. K., Ding, Y. J., Wei, T., and Yu, G. M. (2023). Development adjustment scheme of a low-permeability reservoir in the SN Oilfield. *Energies* 16 (15), 5770. doi:10.3390/en16155770

Xie, L. L., You, Q., Wang, E. Z., Li, T., and Song, Y. C. (2022). Quantitative characterization of pore size and structural features in ultra-low permeability reservoirs based on X-ray computed tomography. *J. Pet. Sci. Eng.* 208, 109733. doi:10.1016/j.petrol.2021.109733

Xu, M. M., Wei, X. C., Yang, R., Wang, P., and Cheng, X. G. (2021). Research progress of provenance tracing method for heavy mineral analysis. *Adv. Earth Sci.* 36, 154–171. doi:10.11867/j.issn.1001-8166.2021.021

Yang, R. C., Fan, A. P., Van Loon, A. J., Han, Z. Z., and Wang, X. P. (2014). Depositional and diagenetic controls on sandstone reservoirs with low porosity and low permeability in the eastern sulige gas field, China. *Acta Geol. Sinica-English Ed.* 88, 1513–1534. doi:10.1111/1755-6724.12315

Yang, X. P., Zhao, W. Z., Zou, C. N., Chen, J. M., and Guo, Y. R. (2007). Origin of low-permeability reservoir and distribution of favorable reservoir. *Actc Pet. Sin.* 28 (4), 57–61.

Yao, H. X., Wang, Z. X., and Zhu, S. Z. (2017). The jurassic fossil-rich clastic sequence and structural response in north of Qaidam Basin. *Northwest. Geol.* 50, 16–27. doi:10.19751/j.cnki.61-1149/p.2017.02.002

Yao, W. L. (2021). Reservoir control of tight sandstone provenance system in Xujiahe Formation, Sichuan Basin. *Bull. Geol. Sci. Technol.* 40, 223–230. doi:10.19509/j.cnki.dzkq.2021.0036

Yi, D. H., Liu, Y. R., Li, J. Y., Liu, J. F., Kui, M. Q., Chen, F. J., et al. (2023). Study on provenance of the quaternary Qigequan Formation in sanhu area, eastern Qaidam Basin. *J. Palaeogeograohy Chin. Ed.* 26, 1–11. doi:10.7605/gdlxb.2024.02.027

Zeng, F. C., Zhang, C. M., Zhu, R., Song, L. Z., Song, W. L., Gao, J., et al. (2023). The main factor influencing reservoir quality of K1yc tight sandstones within volcano-sedimentary succession in the Dehui fault-depression of Songliao Basin, NE China. *Geoenergy Sci. Eng.* 223, 211519. doi:10.1016/j.geoen.2023.211519

Zhang, D. Y. (2017). The research of pore throat characteristics of tight reservoir in jimusar sag. *Xinjiang Geol.* 35, 70–73. doi:10.3969/j.issn.1000-8845.2017.01.011

Zhang, G. Y., Fu, Q., Peng, G. R., Wang, X. D., Zhang, L. L., Xiang, X. H., et al. (2023). Diagenetic evolution and petrophysical characteristics of Paleogene sandstone reservoirs in the southwest baiyun sag, northern south China sea. *Minerals* 13, 1265. doi:10.3390/min13101265

Zhang, W., Jian, X., Fu, L., Feng, F., and Guan, P. (2018). Reservoir characterization and hydrocarbon accumulation in late Cenozoic lacustrine mixed carbonate-siliciclastic fine-grained deposits of the northwestern Qaidam basin, NW China. *Mar. Pet. Geol.* 98, 675–686. doi:10.1016/j.marpetgeo.2018.09.008

Zhang, W. K., Shi, Z. J., Tian, Y. M., Xie, D., and Li, W. J. (2021). The combination of high-pressure mercury injection and rate-controlled mercury injection to characterize the pore-throat structure in tight sandstone reservoirs. *Fault Block Oil Gas Field* 28, 14–20. doi:10.6056/dkyqt202101003

Zhang, Y. Y., Pe-Piper, G., and Piper, D. J. W. (2015). How sandstone porosity and permeability vary with diagenetic minerals in the Scotian Basin, offshore eastern Canada: implications for reservoir quality. *Mar. Pet. Geol.* 63, 28–45. doi:10.1016/j.marpetgeo.2015.02.007

Zhao, D. D., Hou, J. G., Sarma, H., Guo, W. J., Liu, Y. M., Xie, P. F., et al. (2023). Pore throat heterogeneity of different lithofacies and diagenetic effects in gravelly braided river deposits: implications for understanding the formation process of high-quality reservoirs. *Geoenergy Sci. Eng.* 221, 111309. doi:10.1016/j.petrol.2022.111309

Zhao, S. S., Zhang, S. N., and Wan, Y. L. (2015). Feldspar dissolution and its effect on reservoir in kepingtage formation, shuntuoguole low uplift, central Tarim basin. *Petroleum Geol. Exp.* 37 (3), 293–299. doi:10.7603/s40972-015-0045-z

Zheng, J. M., You, J., and He, D. B. (2007). Comparison of control factors for high quality continental reservoirs between bohai bay Basin and Ordos basin. *Geoscience* 21 (2), 376–386.

Zhou, Y., Xu, L. M., Ji, Y. L., Niu, X. B., Che, S. Q., You, Y., et al. (2017). Characteristics and distributing controlling factors of relatively high permeability reservoir: a case study from Chang 8_2 sandstones of Yanchang formation in Longdong area. *Ordos basin. J. China Univ. Min. Technol.* 46 (1), 106–120. doi:10.13247/j.cnki.jcumt.000575

Zhu, X. M., Pan, R., Zhu, S. F., Wei, W., and Ye, L. (2018). Research progress and core issues in tight reservoir exploration. *Earth Sci. Front.* 25 (2), 141–146. doi:10.13745/j.esf.2018.02.015

Zou, C. N., Tao, S. Z., Zhang, X. X., He, D. B., Zhou, C. M., and Gao, X. H. (2009). Geologic characteristics, controlling factors and hydrocarbon accumulation mechanisms of China's Large Gas Provinces of low porosity and permeability. *Sci. China* 39 (11), 1607–1624.

Zou, C. N., Yang, Z., Zhu, R. K., Zhang, G. S., Hou, L. H., Wu, S. T., et al. (2015). Progress in China's unconventional oil and gas exploration and development and theoretical technologies. *Acta Geol. sinca.* 89, 979–1007.

Zou, C. N., Zhang, G. S., Yang, Z., Tao, S. Z., Hou, L. H., Zhu, R. K., et al. (2013). Concepts, characteristics, potential and technology of unconventional hydrocarbons: on unconventional petroleum geology. *Petrol. explor. Dev.* 40 (4), 413–428. doi:10.1016/S1876-3804(13)60053-1